Single dopaminergic neuron DAN-c1 in *Drosophila* larval brain mediates aversive olfactory learning through D2-like receptors

Cheng Qi, Cheng Qian[#], Emma Steijvers[#], Robert A. Colvin, Daewoo Lee*

Department of Biological Sciences, Ohio University, Athens, OH 45701, USA

*Correspondence: leed1@ohio.edu (DL)

[#]Present address:
School of Medicine, Johns Hopkins University, Baltimore, Maryland 21205, USA (CQ);
Department of Physiology, Development and Neuroscience, University of Cambridge, Cambridge CB2 3EL, UK (ES)

Abstract

The intricate relationship between the dopaminergic system and olfactory associative learning in *Drosophila* has been an intense scientific inquiry. Leveraging the formidable genetic tools, we conducted a screening of 57 dopaminergic drivers, leading to the discovery of DAN-c1 driver, uniquely targeting the single dopaminergic neuron (DAN) in each brain hemisphere. While the involvement of excitatory D1-like receptors is well-established, the role of D2-like receptors (D2Rs) remains underexplored. Our investigation reveals the expression of D2Rs in both DANs and the mushroom body (MB) of third instar larval brains. Silencing D2Rs in DAN-c1 via microRNA disrupts aversive learning, further supported by optogenetic activation of DAN-c1 during training, affirming the inhibitory role of D2R autoreceptor. Intriguingly, D2R knockdown in the MB impairs both appetitive and aversive learning. These findings elucidate the distinct contributions of D2Rs in diverse brain structures, providing novel insights into the molecular mechanisms governing associative learning in *Drosophila* larvae.

Key Words:

Drosophila larval aversive learning, D2R, DAN-c1, mushroom body, thermogenetics, optogenetics.

36 **Introduction**

37 Learning defines a behavioral change that results from acquiring information about the
38 environment, and memory refers to the process by which the information is encoded, stored,
39 and later retrieved. Learning and memory forms the basis for higher brain functions, including
40 cognition and decision making, which shapes our individuality[1]. On the cellular and physiological
41 level, learning and memory is achieved by neuroplastic changes in circuits, including neuronal
42 excitability and synaptic plasticity. Usually distinct types of neurotransmitters, such as dopamine,
43 modulate these changes.

44 Dopamine (DA) plays an important role in many mammalian brain functions, including
45 motor functions, motivation, reinforcement, addiction, and learning and memory[2-4].
46 Dopaminergic neurons (DAN) are mainly located in the mesencephalon: DANs in the substantia
47 nigra (SN) are responsible for motor functions, while those in the ventral tegmental area (VTA)
48 are important in reward, addiction, learning and memory[3,5]. Dopamine achieves its functions via
49 two families of G protein-coupled receptors (GPCR): excitatory D1-like and inhibitory D2-like
50 receptors[4]. All D1-like receptors are located post-synaptically; in contrast, D2-like receptors both
51 function post-synaptically and play an important presynaptic role, regulating dopamine release
52 through negative feedback[4]. All these receptors are important in mammalian associative
53 learning[6,7]. D1-like receptors elevate intracellular cAMP by activating adenylyl cyclase (AC) via
54 $G\alpha_s$, while D2-like receptors repress cAMP by inhibiting AC via $G\alpha_{i/o}$. cAMP activates protein
55 kinase A (PKA), leading to the phosphorylation of DARPP-32 (dopamine and cyclic AMP-regulated
56 phosphoprotein, 32kDa), ion channels, and CREB (cAMP response element-binding protein). In
57 addition, dopamine receptors also activate the PLC-PKC, MAPK, and CaMKII pathways[2-4,8-10].

58 Although mammalian studies reveal mechanisms more relevant to human beings, the
59 complexity of the nervous system impedes our understanding about the basic or more universal
60 principles of learning and memory applicable generally to all nervous systems[11]. With a simple
61 central nervous system (CNS) and powerful genetic tools, the fruit fly *Drosophila melanogaster*
62 has become a popular model organism in learning and memory research[12,13]. With conserved
63 genes in dopamine metabolism and signaling[14], as well as fundamental similarities in the
64 olfactory circuitry compared to mammals[15,16], *Drosophila* can perform olfactory associative
65 learning in both larvae[17-19] and adults[20-24]. Olfactory associative learning is a type of classical
66 conditioning in which flies are trained under positive or negative reinforcement paired with an
67 odorant. Different from the naïve reaction to the odorant, flies approach the odorant after being
68 trained with rewards (e.g., sucrose; appetitive)[21], but avoid the odorant when trained with
69 punishments (e.g., electric shock, bitter taste chemicals; aversive)[20]. Several genes related to the
70 cAMP-PKA signaling pathway, including *dunce* (*dnc*)[25] and *rutabaga* (*rut*)[21], are expressed in the
71 mushroom body (the center for *Drosophila* learning and memory)[26,27]. Mutations of these genes
72 lead to learning deficiencies, indicating their roles in olfactory learning[21,25].

73 *Drosophila* larvae offer several advantages for studying olfactory learning compared to
74 adults. Notably, compared to neural circuits underlying olfactory learning, their simpler neural
75 circuitry[28], characterized by fewer olfactory receptor neurons (ORNs)[29,30], projection neurons
76 (PNs) [31], mushroom body neurons (MBNs)[32], and dopaminergic neurons (DANs)[33,34], facilitates
77 the elucidation of underlying mechanisms. Additionally, larvae exhibit simpler behavioral
78 patterns, facilitating experimental manipulations and observations. Furthermore, their

79 translucent cuticles enable convenient application of techniques such as optogenetics[35], further
80 enhancing the experimental versatility of larval studies.

81 Like in mammalian brains, dopamine achieves its functions via four dopamine receptors in
82 flies, two D1-like receptors dDA1[36] (or Dop1R1) and DAMB[37] (or Dop1R2), one D2-like receptor
83 D2R[38] (or Dop2R), and one non-canonical receptor DopEcR[14,39]. dDA1 is mainly found in the
84 mushroom body[40,41] and is necessary for appetitive and aversive olfactory learning in larvae and
85 adults[41,42]. D2R in the mushroom body is necessary for anesthesia-resistant memory[43]. In
86 addition, D2R in GABAergic anterior paired lateral (APL) neurons is known to secure aversive
87 conditioning in adult flies[44]. Although D2R expression has been reported in the ventral nerve
88 cord[45], neither its expression in larval brains, nor its functions in larval olfactory learning have
89 been investigated.

90 By using a GFP-tagged D2R strain, we detected the expression pattern of D2R in the third-
91 instar larval brain, specifically in dopaminergic and mushroom body neurons. Knockdown of D2Rs
92 in DAN-c1 impaired aversive learning, while knockdown of D2R in mushroom body neurons led
93 to deficits in both aversive and appetitive learning. These results revealed that D2Rs in distinct
94 brain structures mediate different learning tasks. The newly discovered roles of D2R in the larval
95 brain provides new insights into the mechanisms underlying larval associative learning.

96 **Results**

97 **Distinct dopaminergic neurons innervate different compartments of the mushroom body.**

98 The connectome of larval learning has been investigated in both first- and third-instar
99 larvae[28,46]. The mushroom body works as the learning center in *Drosophila*, which is composed
100 by αβ, α'β', and γ neurons in adult brains[47]. In larvae, axons from γ neurons bifurcate and form
101 the vertical and medial lobes, as αβ and α'β' neurons are not mature[33,48,49]. These lobes are
102 divided into 11 compartments (refer to Figure 1) based on the coverage of neurites from both
103 mushroom body extrinsic neurons (MBEN) and mushroom body output neurons (MBON)[28].
104 Around 21 dopaminergic neurons are found in each brain hemisphere, and categorized into 4
105 clusters: DM1 (dorsomedial), pPAM (primary protocerebral anterior medial, or DM2)[50], DL1
106 (dorsolateral), and DL2[34]. DL1 neurons project to the vertical lobe[41], while pPAM neurons
107 innervate the medial lobe[50] (refer to Figure 1a-c).

108 In this study, we wanted to functionally identify individual DANs that mediate larval olfactory
109 learning. The first step was to search for DAN-specific driver strains that mark single
110 dopaminergic neurons, which subsequently can be used to target genetic manipulations of
111 corresponding neurons. A total of 56 driver strains identifying dopaminergic neurons were
112 screened in this study (Table 1). These strains were chosen based on previous studies, either
113 identifying a single dopaminergic neuron in larvae, or identifying only several in adult brains and
114 indicating the potential of identifying single DAN in larvae. TH-GAL4, a traditional dopaminergic
115 neuronal driver[51], identifies all dopaminergic neurons except those in pPAM (Figure 1d, Figure
116 S1a). Split-GFP reconstitution across synaptic partners (GRASP) technique was used to investigate
117 the "direct" synaptic connections from DANs to the mushroom body (MB), in which portions of

118 GFP were specifically expressed in corresponding neurons (Figure S2d). GRASP results showed
119 neurons under TH-GAL4 formed synapses in the vertical lobe and lower peduncle (white dash
120 lines in Figure 1d'), consistent with previous electron microscopy data[46]. We found three DAN
121 driver strains that identify single dopaminergic neurons in the third-instar larval brain
122 hemisphere. DAN driver R76F02-AD;R55C10-DBD identifies a dopaminergic neuron innervating
123 the lower peduncle (LP), which would be DAN-c1 based on previous published nomenclature[28]
124 (Figure 1f). MB296B driver identifies the dopaminergic neuron (DAN-d1) projecting to the lateral
125 appendix (LA) (Figure 1g), as well as many non-dopaminergic neurons. SS1716 driver identifies
126 one dopaminergic neuron forming synapses in the lower vertical lobe (LVL), indicating it is DAN-
127 g1 (Figure 1h).

128 In pPAM, R58E02 driver identifies DAN-h1, i1, and j1, innervating the shaft (SHA),
129 intermediate toe (IT) and upper toe (UT) (Figure 1i), and R30G08 driver identifies DAN-h1 and i1
130 (Figure 1j). As described in a previous report[28], SS864 driver identifies DAN-i1, innervating the
131 upper toe (Figure 1l), and SS1757 driver identifies DAN-k1 which innervates the lower toe (LT)
132 (Figure 1m). In contrast, SS1696 driver identifies not only DAN-h1, but also i1 and one DL1 neuron
133 not innervating the mushroom body (Figure 1K).

134 In summary, our results show that five DL1 and four pPAM DANs innervate nine distinct
135 mushroom body compartments in a one-to-one pattern (Figure 1b and c). DL1 neurons innervate
136 the vertical lobe and peduncle, while pPAM neurons project to the medial lobe. The single
137 neuronal driver strains screened can be used to investigate the roles of individually identified
138 DANs in larval olfactory learning.

139

140 **Dopamine release from DAN-c1 is both necessary and sufficient for larval aversive learning.**

141 Dopamine plays an important role during olfactory associative learning in both adults and
142 larvae[52,53]. In adults, dopaminergic neurons in PPL1 regulate aversive learning[54-57], while those in
143 PAM mediate reward signals in appetitive learning[58-60]. In larvae, DL1 neurons innervating the
144 vertical lobe and the peduncle are required for aversive learning[18,41], while those in pPAM
145 projecting to the medial lobe are involved in appetitive learning[50].

146 In Figure 1 and Table 1, three driver strains identifying single dopaminergic neurons in DL1
147 were discovered, which could be candidates to investigate their roles in larval aversive learning.
148 The R76F02-AD;R55C10-DBD strain identifies MB-MP1 in the adult brain[61], which is a
149 dopaminergic neuron involved in adult aversive learning[62]. This driver strain identifies one
150 neuron per hemisphere in the third-instar larval brain (Figure 2a-c, Figure S1c). Using a UAS-
151 DenMark;UAS-sytGFP strain, its dendrites were labeled with RFP and axonal terminals were
152 marked by GFP. Its dendrites were localized in the dorsomedial protocerebrum (dml), and its
153 axonal terminals located in the lower peduncle of the mushroom body (Figure 2a and d), with
154 GRASP results supporting the existence of synapses in this compartment (Figure 2E). All these
155 characteristics are consistent with the previously published nomenclature[28], indicating that this
156 neuron is DAN-c1 (Figure 2f), thus, this strain will now be referred to simply as DAN-c1.

157 To reveal the role of DAN-c1 in larval olfactory learning, a single odor learning paradigm and
158 thermogenetic tools were applied[17,18,63]. Compared to those trained with distilled water (DW),
159 control larvae exhibited repulsion to the odorant pentyl acetate (PA) after being trained with
160 quinine (QUI) paired with PA, reflecting aversive learning. In contrast, larvae were attracted to
161 PA after being trained with sucrose (SUC) paired with PA, reflecting appetitive learning. The

162 extent of repulsion or attraction was represented with a response index (R.I.) that is compared
163 to the DW group (Figure 2g).

164 To examine the role of DAN-c1 in aversive learning, we used a *Shibire*^{ts1} strain, which
165 encodes a thermosensitive mutant of dynamin blocking neurotransmitter release when the
166 ambient temperature is higher than 30°C by repressing endocytosis and vesicle recycling
167 functions[17]. When trained at 34°C, the complete inactivation of dopamine release from DAN-c1
168 with *Shibire*^{ts1} impaired aversive learning (Figure 2h), while *Shibire*^{ts1} did not affect learning when
169 trained at room temperature (22°C). These data indicated that dopamine release from DAN-c1 is
170 necessary for larval aversive learning to occur.

171 In the next experiments, a fly carrying temperature-sensitive cation channel, dTRPA1, was
172 used to excite the DAN-c1 neuron because it can be activated at temperatures higher than 30°C[58].
173 Activation of DAN-c1 with dTRPA1 at 34°C during training induced repulsion to PA in the distilled
174 water group (Figure 2k). These data suggested that DAN-c1 excitation and presumably increased
175 dopamine release is sufficient for larval aversive learning in the absence of gustatory pairing.

176 Combining the blockade results with *Shibire*^{ts1}, these data revealed that dopamine released
177 from DAN-c1 activation is both necessary and sufficient in larval aversive learning. However,
178 when paired with a gustatory stimulus (QUI or SUC), activation of DAN-c1 during training impairs
179 both aversive and appetitive learning (Figure 2k). We suggest that these data indicate a critical
180 role for the amount of DAN-c1 dopamine release in larval associative learning, as dTRPA1
181 stimulation may result in excessive dopamine release.

182

183 **The expression pattern of D2R in the third-instar larval brain.**

184 Although dopamine D1-like receptors have been proven important for learning[42], the role of
185 D2-like receptors has not been fully investigated. In addition, the expression pattern of D2R in fly
186 brains was not reported. A fly strain expressing GFP-tagged D2R (BDSC#60276) was used to reveal
187 the expression pattern of D2R in the third-instar larval brain (Figure 3a). D2Rs were found in
188 dopaminergic neurons and the mushroom body. In dopaminergic neurons (Figure 3b-g), D2Rs
189 were found in DM1, pPAM, DL2b, and some DL1 neurons. In the mushroom body, D2Rs were
190 expressed in the soma and lobes, but not in the calyx (Figure 3h and i). Even though D2Rs were
191 widely found in vertical lobes, medial lobes, and peduncles, they were not expressed in every
192 mushroom body neuron. A transection of the peduncle region showed the absence of D2Rs in
193 the core area (Figure S3i), which is composed of densely packed newly created fibers and lacks
194 Fasciclin II (FAS II)[49].
195 To inspect whether the pattern of GFP signals indeed reflected the expression of D2R, three
196 D2R enhancer driver strains (R72C04, R72C08, and R72D03-GAL4) were crossed with the GFP-
197 tagged D2R strain. R72C08-GAL4 covered three DM1 dopaminergic neurons (Figure S3c), and
198 R72C04-GAL4 labeled one DM1 and two DL2b dopaminergic neurons (Figure S3d and e). R72D03-
199 GAL4 identified parts of mushroom body neurons, whose axons spread on the surface of the
200 mushroom body lobes (Figure S3f); R72C08-GAL4 also identified a subset of neurons from four
201 MB neuroblasts, with soma in four clusters and a converged bundle of axons (Figure S3g and h).
202 These results revealed the expression of D2R in the mushroom body and dopaminergic neurons
203 in the third-instar larval brain.
204
205 **D2R in DAN-c1 influences larval aversive learning.**

206 Our previous work reported that D2R knockdown (UAS-RNAi) in dopaminergic neurons
207 driven by TH-GAL4 impaired larval aversive learning[63]. Using a microRNA strain (UAS-D2R-miR)[61],
208 a similar deficit was observed (Figure S5c). To further understand the roles of D2R in aversive
209 learning, its expression in distinct DANs, as well as corresponding learning assays were both
210 investigated. Crossing the GFP-tagged D2R strain with a DAN-c1-mCherry strain demonstrated
211 the expression of D2R in DAN-c1 (Figure 4a).

212 To reduce the expression of D2R in dopaminergic neurons, a microRNA strain UAS-D2R-miR
213 was used when crossing with distinct driver strains. The efficiency of D2R knockdown was
214 confirmed by crossing the GFP-tagged D2R strain with TH-GAL4;UAS-D2R-miR. In these larval
215 brains, GFP signals in DM1 were not detected, while those in pPAM were still intact (Figure 4b
216 and c). Quantification showed a significant decrease of GFP signals in the knockdown group
217 compared to the control (Figure 4d), indicating reduced transcripts of D2R linked GFP by D2R-
218 microRNA (Figure S4f).

219 To investigate the roles of D2R in distinct dopaminergic neurons during larval associative
220 learning, UAS-D2R-miR strain was crossed with distinct single dopaminergic neuronal drivers.
221 Among them, the knockdown of D2R in DAN-c1 impaired aversive learning with the odorant
222 pentyl acetate, while appetitive learning was unaffected (Figure 4e). In contrast, although D2R
223 was also found in DAN-d1 and DAN-g1, neither D2R knockdown in DAN-d1 nor in DAN-g1 affected
224 larval olfactory learning (Figure S4c-e). As the naïve sensory and motor functions were not
225 affected, this deficiency was caused by impairment in learning abilities (Figure 4f-i). Similar
226 learning deficits were observed in the same strain trained with another odorant, propionic acid
227 (Figure S5a), as well as in larvae with D2R knockdown using UAS-RNAi (Figure S5b). These results

228 demonstrated that D2Rs are expressed in DAN-c1, and they are necessary for larval aversive
229 learning. Presumably the knockdown of presynaptic inhibitory D2R autoreceptors on DAN-c1 will
230 result in increased and excessive dopamine release, which leads to aversive learning deficiency.
231 These results are consistent with the activation studies with dTRPA1 above, in which increased
232 dopamine release during training results in impaired aversive learning (Figure 2k).
233
234 **Over-excitation of DAN-c1 during learning impairs larval aversive learning.**
235 To exclude possible chronic effects of D2R knockdown during development, optogenetics
236 was applied at distinct stages of the learning protocol. Channelrhodopsin2 (ChR2) is a blue light
237 activated cation channel from algae, which can be used to activate target neurons[64,65]. Over-
238 excitation of DANs under a TH-GAL4 driver with ChR2 during training impaired aversive learning
239 but left appetitive learning intact (Figure S7), which is consistent with D2R knockdown results. To
240 investigate the mechanisms with a better temporospatial resolution, ChR2 was expressed in
241 DAN-c1, and blue light was applied at distinct stages of the learning protocol (Figure 5a).
242 Optogenetic activation of DAN-c1 during training impaired aversive learning, not appetitive
243 learning (Figure 5b-d). This result is consistent with the effect of D2R knockdown in DAN-c1,
244 indicating that increased, excessive dopamine release during training leads to impaired aversive
245 learning.
246
247 **D2R in mushroom body mediates larval learning through inhibition.**
248 We have shown that D2R in DAN-c1 plays a critical role in larval aversive learning. Since D2Rs
249 are also expressed in soma and axons in most mushroom body neurons (Figure 3h and i), we

250 examined the role of D2R in MB neurons, the center for learning in *Drosophila*. Knockdown of
251 these D2Rs by D2R-miR impaired both appetitive and aversive learning (Figure 6a). Similarly,
252 optogenetic activation of mushroom body neurons during training led to deficiencies in both
253 appetitive and aversive learning (Figure 6b and d). These deficiencies were not observed in larvae
254 with activation during the resting stage. As D2Rs are inhibitory receptors, and optogenetic
255 activation leads to greater neuronal excitation like what may occur with knockdown of D2Rs,
256 these data show that the inhibitory effect of D2Rs in mushroom body neurons is necessary for
257 larval olfactory associative learning to occur.
258
259
260 **Discussion**
261 The dopaminergic system plays an important role in *Drosophila* olfactory associative
262 learning, but the roles of D2R in this process have not been fully explored. In this study, we
263 systematically investigated the expression pattern of D2R in the third-instar larval brain as well
264 as its role in larval aversive and appetitive learning. One driver strain singly identifying the DAN-
265 c1 neuron was discovered and learning assays with thermogenetic tools (*Shibire*^{ts1}, dTRPA1)
266 determined that the blockade of dopamine release from DAN-c1 impeded aversive learning,
267 while its activation during training led to repulsion toward the odor in the absence of
268 unconditioned stimulus (i.e., QUI). These results revealed that DAN-c1 activation (i.e.,
269 presumably leading to the release of synaptic dopamine) is both necessary and sufficient for
270 larval aversive learning to occur. Subsequently, the expression pattern of D2R was explored by
271 using a GFP-tagged D2R strain, including distinct dopaminergic and mushroom body neurons.

272 D2Rs were expressed in DAN-c1, and the knockdown of these receptors resulted in aversive
273 learning deficiency. These data suggest that presynaptic D2Rs in a single dopaminergic neuron,
274 DAN-c1, regulate dopamine release during excitation whereas knockdown of these same
275 receptors leads to excessive dopamine release, causing deficits in aversive learning to occur.
276 Furthermore, the activation of DAN-c1 with optogenetic tools during training, resulting in
277 excessive dopamine release, impaired aversive learning, as well. Finally, it was demonstrated that
278 either the knockdown of postsynaptic D2R or activation of mushroom body neurons led to
279 learning deficits. These data demonstrate that D2Rs in distinct brain locations are critically
280 involved in associative learning.
281
282 **Insights into the neuronal circuits underlying larval olfactory associative learning.**
283 Mushroom body and dopaminergic neurons play important roles in *Drosophila* associative
284 learning[66-69]. In larvae, olfactory information (odors, Conditioned Stimulus, CS) is received by
285 olfactory sensory neurons (OSN), then transmitted to the mushroom body via projection neurons
286 (PN)[70]. The mushroom body (MB) is the learning center of *Drosophila* and composed of Kenyon
287 cells (KC, or mushroom body neurons, MBN)[71-73]. Their dendrites form the calyx, receiving
288 olfactory information from projection neurons. The axons converge into peduncles, then branch
289 into the vertical and medial lobes. Distinct gustatory cues (taste, Unconditioned Stimuli, US) are
290 sensed by gustatory sensory neurons (GSN) and transferred to dopaminergic neurons in different
291 clusters (Figure 7A). DAN-c1 in the DL1 cluster mediates aversive cues, projects to the lower
292 peduncle (LP) in the mushroom body. The plasticity of synapses from MBNs to MB output
293 neurons (MBON) is negatively modulated by dopamine[67,74,75]. The MBN-MBON synapses in the

294 vertical lobe and peduncle are responsible for attraction, while those in the medial lobe are for
295 repulsion[67,75].

296 When only the odorant appears, the subset of Kenyon cells representing this odor are
297 depolarized, inducing calcium influx[73]. As a balance exists between compartments across the
298 mushroom body lobes, the response to the odor depends on the naïve olfactory circuits from
299 projection neurons to the lateral horn (LH). In aversive learning, in addition to olfaction induced
300 calcium influx, gustatory stimuli also lead to dopamine release from DAN-c1 and subsequently,
301 activation of $G\alpha_s$ in LP[54]. The co-existence of calcium and $G\alpha_s$ activates a Ca^{2+}-dependent
302 adenylate cyclase (AC), rutabaga (rut)[76-79]. Rutabaga converges information from both olfaction
303 and gustation, working as the coincidence detector of associative learning. Its downstream
304 signaling inhibits attractive MBN-MBON synapses in the LP, breaking the balance between
305 distinct compartments. As a result, after learning, the larvae will exhibit repulsion when exposed
306 to the odor again. In contrast, dopaminergic neurons in the pPAM convey appetitive cues, which
307 project to compartments in the medial lobe. The co-existence of olfactory and appetitive
308 gustatory stimuli leads to inhibition of these repulsive MBN-MBON synapses, inducing attraction.
309

310 **The conserved role of DAN-c1 in aversive learning throughout *Drosophila* development.**

311 Adult *Drosophila* share similar neuronal circuits of learning with larvae[54,66-69]. In adult brains,
312 dopaminergic neurons are classified into 13 clusters, named as PAM (protocerebral anterior
313 medial), PAL (protocerebral anterior lateral), PPM (protocerebral posterior medial), PPL
314 (protocerebral lateral), and PPD (protocerebral posterior dorsal) clusters[32]. DANs in the PAM
315 cluster innervate the medial lobe, while those in PPL1 project to the vertical lobe[69].

316 R76F02-AD;R55C10-DBD identifies two dopaminergic neurons in adult brains, MB-MP1 in
317 PPL1 and ALT-PLPC in PPL2ab [61]. MB-MP1 is also named PPL1-γ1pedc, innervating both γ1 and
318 the peduncle of the β lobe[69]. Activation of this neuron induced aversive learning[62], and activation
319 of its corresponding MBON-γ1pedc>α/β led to approach[80]. During metamorphosis, dopaminergic
320 neurons in DL1 develop into the PPL1 cluster, DL2a neurons develop into PPL2ab, and those in
321 pPAM will develop into the PAM cluster[81]. This driver strain only identifies DAN-c1 from DL1 in
322 larvae, which innervates the lower peduncle of the mushroom body. Interestingly, previous
323 reports revealed that memory can be transferred from larvae to adults[82], indicating the
324 maintenance of neuronal circuitry architecture during metamorphosis. This evidence supports
325 that DAN-c1 is the corresponding neuron of PPL1-γ1pedc in larvae, which performs similar
326 functions in aversive learning.
327
328 **Pre- and post-synaptic D2Rs regulate cAMP in the mushroom body during aversive learning.**
329 The molecular mechanisms underlying *Drosophila* learning have not been fully determined.
330 In a traditional view, gustatory cues elevate dopamine release, which binds to D1 receptors and
331 then activates $G\alpha_s$. The co-existence of $G\alpha_s$ and calcium elicited by olfactory cues activates
332 rutabaga in axons of MBNs. Rutabaga transforms ATP into cAMP, activating PKA signaling
333 pathway. Mutant flies with either insufficient (*rutabaga*) or excessive cAMP (*dunce*) showed
334 aversive learning deficiency, indicating that the level of cAMP should be kept in an optimal range
335 to achieve aversive learning[21,25] (Figure 7B).
336 Our results have shown that D2Rs in dopaminergic neurons and the mushroom body are
337 important for larval aversive learning, suggesting a "*dual brake*" role in regulating cAMP levels in

338 the MBNs through both pre- and postsynaptic components. On the presynaptic side, D2R in DAN-
339 c1 decreases the release of dopamine under gustatory stimuli, reducing the probability of
340 postsynaptic D1R activation in MBNs. On the postsynaptic side, D2R in MBNs inhibits the
341 coincidence detector rutabaga (AC) both via activation of $G\alpha_{i/o}$ and inhibition of voltage-gated
342 calcium channels[2], indicating postsynaptic D2R functioning as a "*brake of the coincidence*
343 *detector*". Combining these, "*dual brake*" D2R ultimately regulates the mushroom body cAMP
344 level within a physiologically optimal range during aversive learning. In addition, D2R fine tunes
345 the functional concentration spectrum of dopamine with higher resolutions, as its dopamine
346 affinity is 10- to 100-fold greater than D1 receptors. Overall, D2Rs work in a "dual brake" system
347 both expanding the representation of a dynamic range of gustatory signal intensity with high
348 signal to noise ratio and preventing postsynaptic overexcitation, which increases the reliability of
349 DAN-c1 and MBN circuits for the larval aversive learning (Figure 7C & D).

350 Recent studies showed that the approach/repulsion in learning is achieved via inhibition of
351 the repulsive/attractive representing compartments[67,74,75], which indicates dopamine inhibits
352 acetylcholine release from MBN to MBON[83]. However, the PKA signaling pathway usually
353 elevates neuronal excitability and increases neurotransmitter release[2,3], which is contradictory
354 to the recent findings. In addition to the "*dual brake*" role of D2R, our results suggest a third role
355 of D2R in aversive learning. D1 and D2 receptors can form heteromeric receptors, whose
356 downstream $G\alpha_q$ activates PKC and CaMKII signaling pathways. The activation of these signaling
357 pathways may reduce acetylcholine release[84] (Figure 7C & D).

358

359 **Explaining the results of thermogenetic and optogenetic experiments.**

360 Activation of DAN-c1 with dTRPA1 induced aversive learning, while the repulsion
361 disappeared when DAN-c1 was activated in the quinine group (Figure 2K). Our explanation is that
362 quinine stimulation and temperature activation led to over-excitation of DAN-c1, which impaired
363 aversive learning. This is consistent with the learning deficiency in larvae with D2R knockdown in
364 DAN-c1 (Figure 4E). Results from optogenetic activation of DAN-c1 during aversive learning also
365 support this (Figure 5B). However, in contrast to results with thermo-activation, larvae with
366 optogenetic activation of DAN-c1 showed neither repulsion after being trained with distilled
367 water (Figure 5C), nor did they show reduced attraction in the sucrose group (Figure 5D). One
368 possible explanation is that the thermo-activation is relatively mild compared to the optogenetic
369 activation. Based on this, thermo-activation of DAN-c1 is still in the physiological range of cAMP
370 under the upper cutoff (Figure 7B), resulting in repulsion in the distilled water (DW) group,
371 neutralized attraction in SUC group, and impaired repulsion in QUI group. In contrast,
372 optogenetic activation of DAN-c1 overwhelmed the physiological conditions, leading to failure of
373 repulsion in DW group (Figure 5C). This repulsive failure did not affect appetitive learning (Figure
374 5D), and a stronger over-excitation in QUI group induced similar failure (Figure 5B).
375
376 **Distinct dopaminergic neurons may have different roles in larval aversive learning.**
377 Previous work reported that aversive olfactory learning was induced through the optogenetic
378 activation of DAN- d1, f1, or g1, but not DAN-c1[85]. This discrepancy can be explained as the
379 optogenetic overexcitation of DAN-c1, similar to our optogenetic or D2R knockdown results. Our
380 learning assay results from larvae with D2R knockdown in DAN-d1 or g1 also supported this:
381 aversive learning was not affected by D2R knockdown (Figure S4E). These data indicate D2Rs in

382 DAN-d1 or g1 are not involved in larval aversive learning. Additionally, the DAN-c1 strain used in
383 the previous work (SS02160-split-GAL4) not only labels DAN-c1, but also marks other non-
384 dopaminergic neurons, which may affect the results. Besides, live calcium imaging showed that
385 DAN-d1, f1, and g1 responded to the activation of mechanosensory and nociceptive neurons[85],
386 indicating a functional differentiation from gustatory activated DAN-c1[62,86].

387 In future studies, the molecular signaling downstream of D2R needs to be explored, as well
388 as the comprehensive neuronal circuit architectures of larval learning. The neuronal circuits
389 underlying learning and memory are complex networks, sharing similarities with the regulatory
390 networks of gene expression. Studies of the mechanisms of learning and memory help us
391 understand the essential principles of the non-linear dynamic characteristics in these complex
392 systems. On one hand, the progress in larval learning provides useful information for helping our
393 understanding about more complex systems, from brains in adult flies to those in mammals. On
394 the other hand, the architecture of larval learning circuits could improve either hardware design
395 or algorithm structures in artificial intelligence, which may bring more powerful tools, such as
396 navigation systems regulating multiple auto-drive vehicles in complex 3-dimentional
397 environments.

398 In conclusion, we explored the expression pattern of D2R in the third-instar larval brain and
399 investigated their roles during larval olfactory learning. D2Rs were found in DAN-c1, and their
400 knockdown induced deficiency in aversive learning. D2Rs were also expressed in MBNs,
401 knockdown of which impaired both aversive and appetitive learning. This research revealed the
402 important roles of D2Rs in *Drosophila* larval olfactory learning and enriched our understanding
403 regarding the mechanisms underlying the learning process.

404 **Materials and Methods:**
405

406 ***Fly stocks*** All fly strains used in this study are listed in Table 1 and Table S1. Flies were
407 maintained on standard medium, which consists of cornmeal, yeast, dextrose, sucrose and agar
408 in water. Flies were kept in a 12/12-hour light/dark cycle at 25℃. Canton-S genotype (WT) and
409 yw^{1118} were used as wild-type. Strains carrying more than one transgene were constructed by
410 standard genetic crosses with the w^{1118}; CyO/Sco; TM2/TM6 multiple balancer chromosome
411 strain. Strain UAS-Syb::spGFP1-10, LexAop-CD4::GFP11, LexAop-rCD2::RFP /CyO; MB247-
412 LexA::Up16/TM6B was made by chromosome swapping between UAS-Syb::spGFP1-10, LexAop-
413 CD4::GFP11/CyO (II, second chromosome) and LexAop-rCD2::RFP (II).
414 The D2R gene is located on the X chromosome, with 6 different alternative splicing products.
415 The GFP-tagged D2R strain is inserted with a GFP gene in the second intron, generating D2R
416 molecules tagged with GFP[87,88]. The D2R-miR strain produces microRNA recognizing the
417 sequence across the third and fourth exons, which is not affected by the GFP insertion (Figure
418 S4F).
419 ***GRASP*** Split-GFP reconstitution across synaptic partners (GRASP) was used to investigate
420 whether neurons formed synapses[89] (Figure S2d). Half of split GFP tethered to the presynaptic
421 synaptobrevin (UAS-syb::spGFP1-10) was expressed in one type of neuron using UAS/Gal4 binary
422 system, and the complementary split GFP linked to a membrane protein (LexAop-CD4::spGFP11)
423 was expressed in another category of neuron with LexA/LexAop. If synapses between these
424 neurons exist, the split GFPs would form a complete one and be recognized by a mouse antibody
425 (Figure S2a-c).

426 ***Immunohistochemistry*** All staining processes were performed in 1.5 ml Eppendorf tubes. Late
427 third-instar (96-100h after egg laying) larval brains were dissected in dissection solution (300
428 mOsmol/L). Brains were fixed in 4% paraformaldehyde (PFA, Electron Microcopy Sciences, Cat.
429 No. 15713) for 1 hour on ice. After three washes (0.1% bovine serum albumin in 10mM PBS,
430 Sigma Life Sciences A9647), brains were incubated in the blocking and permeabilization solution
431 (0.2% Triton X-100 in 10mM PBS with 5% normal goat serum; Triton-X 100, Sigma, T8532; NGS,
432 Sigma-Aldrich, G9023) for 2 hours at room temperature. Incubation with primary antibodies was
433 done overnight at 4°C. After three washes, brains were incubated in the secondary antibodies
434 for two hours. Both the primary and secondary antibodies were diluted in the blocking and
435 permeabilization solution. GFP antibody (Rabbit, Thermo Fisher Scientific, Cat. No. A6455,
436 1:1000), TH antibody (Mouse, Immunostar, Cat. No. 22941, 1:1000), goat anti-rabbit with green
437 fluorescence (Invitrogen, Alexa Fluor 488 conjugate, Cat. No. A-11035, 1:1000), and goat anti-
438 mouse IgG with far-red fluorescence (Alexa Fluor 633 conjugate, Cat. No. 21052, 1:500)
439 secondary antibodies were used. After three washes, brains were transferred and mounted in
440 the Fluoro-Gel with Tris Buffer (Electron Microcopy Sciences, Cat. No. 17985-10) on a piece of
441 micro cover glasses (Electron Microcopy Sciences, Cat. No. 72200-41). Finally, the samples were
442 covered with another piece of micro cover glasses.

443 A seven-day staining protocol was used for staining of GFP-tagged D2R or GRASP, in which
444 brains were fixed in 1% paraformaldehyde in Schneider's insect medium (Sigma Life Sciences,
445 Cat.NO. S0146) overnight at 4°C. In the second day, the brains were rinsed and washed twice
446 with PAT3 solution (0.5% Triton X-100 in 10mM PBS with 0.5% BSA), each for 1 hour. Then brains
447 were incubated in the blocking and permeabilization solution (3% NGS in PAT3) for 2 hours at

448 room temperature. Incubation of primary antibodies was done overnight at 4°C. On the third day,
449 brains were rinsed and washed twice with PBT solution, then incubated in the secondary
450 antibodies for five days. Both the primary and secondary antibodies were diluted in the PBTN
451 solution. In the staining of GFP-tagged D2R, GFP antibody (Rabbit, ThermoFisher Scientific, Cat.
452 No. A6455, 1: 1000), TH antibody (Mouse, Immunostar, Cat. No. 22941, 1:1000), and mCherry
453 antibody (Rat, ThermoFisher Scientific, Cat. No. M11217, 1:1000) were used. For staining of
454 GRASP, GFP antibody (Mouse, ThermoFisher Scientific, Cat. No. G6539, 1:100) was used. Goat
455 anti-rabbit with green fluorescence (Invitrogen, Alexa Fluor 488 conjugate, Cat. No. A-11035,
456 1:1000), goat anti-mouse with green fluorescence (Alexa Fluor 488 conjugate, Cat. No. A11029,
457 1:1000), goat anti-mouse with far-red fluorescence (Alexa Fluor 633 conjugate, Cat. No. A21052,
458 1:500), and goat anti-rat with red fluorescence (Alexa Fluor 546 conjugate, Cat. No. A-11081,
459 1:1000) secondary antibodies were used. In the seventh day, brains were rinsed and washed
460 twice with PBT solution, and then transferred and mounted in the Fluoro-Gel with Tris Buffer on
461 a piece of micro cover glasses. Finally, the samples were covered with another piece of micro
462 cover glasses.
463 ***Confocal imaging*** All images were obtained with a Zeiss Laser Scanning Microscope 510 (LSM510,
464 Carl Zeiss, Inc., USA). Under 40× and 100× objective magnifications, images were collapsed from
465 confocal stacks of 1.0 µm optical slices. Under 25× objective magnifications, images were
466 collapsed from confocal stacks of 2.0 µm optical slices. Under 10× objective magnifications,
467 images were collapsed from confocal stacks of 12.5 µm optical slices. ImageJ software was used
468 to remove other signals outside of the mushroom bodies, as the background noise in GRASP is
469 strong.

470 ***Larval olfactory learning assays*** A single odor learning paradigm was slightly modified from
471 previous publication[17,18]. In brief, 25 to 50 third-instar larvae (92–96 h after egg laying) were
472 trained on a 2.5% agar plate (100mm petri dish) covered with 2 mL of 1 M sucrose solution (SUC,
473 Sigma, Cat. No. S1888) or 0.1% quinine hemisulfate solution (QUI, Sigma, Cat. No. 22640).
474 Distilled water (DW) was used as a control. An odorant pentyl acetate (PA, 10μL, Sigma-Aldrich,
475 CAT. No. 109584) was placed on a small piece of filter inside the lid. After 30 minutes, larvae were
476 rinsed and transferred to the middle line of a new 2.5% agar plate. A small piece of filter paper
477 with 2.5μL pentyl acetate was placed on one side of the plate, while distilled water on the other
478 side. After 5 min, the numbers of larvae in the two semicircular areas were counted and the
479 response index (R.I.) was calculated with the following equation (Figure 2g):

480 $$\boldsymbol{R.I.} = \frac{\boldsymbol{\#\ of\ larvae\ on\ odorant\ side\ in\ dashline - \#\ of\ larvae\ on\ DW\ side\ in\ dashline}}{\boldsymbol{Total\ \#\ of\ larvae\ on\ two\ sides\ in\ dashlines}}$$

481 ***Naïve Olfactory Test*** Larvae were transferred into the midline of test plates. 2.5μL of odorant
482 were added on one side and distilled water on the other side. The number of larvae in two
483 semicircular areas were counted and the R.I. was calculated after 5 min.

484 ***Naïve Gustatory Test*** A petri dish with a median separator was used. Both sides were filled with
485 1% agar, with 2 mL of distilled water on the control side, and with 1 M sucrose (SUC) solution, or
486 0.1% quinine hemisulfate (QUI) solution on the test side. Twenty larvae were put on each side
487 near the midline and allowed to move for 5 min. Gustatory R.I. was calculated using the larvae
488 numbers on two sides[90].

489 ***Larval locomotion assay*** Individual larvae were placed on the surface of a plate of 2.5% agar
490 mixed with 1mL India ink. They were allowed to acclimate for 1 min, and then a video was
491 recorded for 30 seconds using a Moticam3 digital camera (Motic) and Motic Images Plus 2.0

492 software. The video was analyzed by the MTrack2 plug-in (from
493 http://valelab.ucsf.edu/~nico/IJplugins/MTrack2.html) in ImageJ. The path was recorded; scores
494 were quantified as the length traveled per minute as previously described[91]. As the locomotion
495 speed of DAN-c1 homozygous was slow, DAN-c1 × WT was used as the control group.

496 ***Learning assays with thermogenetics*** In learning assays with thermogenetics, 25 to 50 third-
497 instar larvae (92–96 h after egg laying) were trained on a 2.5% agar plate (100mm petri dish)
498 covered with 2 mL of 1 M SUC or 0.1% QUI. DW was used as a control. An odorant PA was placed
499 on a small piece of filter inside the lid. Training plates were put in a water bath either under 22°C
500 or 34°C. After 30 minutes, larvae were rinsed and transferred to the testing plate. After 5 min,
501 the response index (R.I.) was calculated.

502 ***Learning assays with optogenetics*** In learning assays with optogenetics, egg laying plates with
503 1mM ATR (all-trans retinal, Sigma, Cat. No. R2500) were used. All-trans retinal (ATR) is a
504 necessary light-isomerizable chromophore for ChR2, which is not synthesized by *Drosophila*.[92,93]

505 Around 50 third-instar larvae were trained in a 35mm petri dish with 2 mL of either 1 M SUC
506 or 0.1% QH solutions. DW was used as a control. During training, an odorant was placed on a
507 small piece of filter inside the lid. To activate channelrhodopsin2, a LED (Luxeon Rebel Color LEDs,
508 07040 PB000-D, wavelength 470 nm) with a power supply (GW Instek, Laboratory DC power
509 supply Model GPS-1830D) was used. The intensity of the blue light was 25 mW, measured by a
510 laser power meter (Sanwa, LP1). After being trained for 30 minutes, larvae were rinsed and
511 transferred to the middle line of a 2.5% agar plate in 100 mm test plate. A small piece of filter
512 paper with pentyl acetate was placed on one side of the plate, while distilled water on the other

513 side. Then the number of larvae in the two semicircular areas were counted and the R.I. was
514 calculated after 5 min.

515 ***Quantification of D2R knockdown*** Quantification of the fluorescent intensity of D2R knockdown
516 was performed as follows. TH signals were used to define dopaminergic neurons, and the mean
517 fluorescent intensity of GFP in each neuron was calculated with subtraction of the background.
518 The mean intensity of DM1 was divided by that of pPAM, and the value in the knockdown group
519 was subsequently normalized with the control group.

520 ***Statistical Analysis*** Information for statistical analysis is provided in figure legends.

521 **Author contributions**

522 **Qi. C.:** Conceptualization, Methodology, Formal analysis, Investigation, Writing – Original
523 Draft, Visualization, **Qian. C.:** Writing – Review & Editing, **Steijvers. E.:** Writing – Review & Editing
524 **Colvin. R.:** Writing – Review & Editing **Lee. D.:** Conceptualization, Writing – Review & Editing,
525 Supervision, Funding acquisition

526

527

528 **Acknowledgements**

529 This work was partially supported by an NIH grant (AG065925) and an International Collaboration
530 Grant from Korea Institute of Science & Technology (Brain Science Institute), Seoul, Korea. CQ
531 was a recipient of the SEA and GSR awards from Ohio University. We thank Dr. J Hirsh (University
532 of Virginia), Dr. M. Wu (Johns Hopkins University), Dr. M. Zlatic and Dr. C. Eschbach (HHMI Janelia
533 Research Campus), Dr. M. Gallio (Northwestern University), Dr. A. Kopin (Tufts-New England
534 Medical Center), Dr. S. Tanda (Ohio University), Dr. B. Condron (University of Virginia), Dr. T.
535 Kitamoto (University of Iowa) for their kind gift strains.

536

537

538 **Declaration of Interest**

539 The authors declare no competing interests.

540

541 **Figure legends**
542
543
544 **Figure 1. Identification of driver strains for single dopaminergic neurons in the *Drosophila***
545 **larval brain. (a)** A schematic diagram shows the dopaminergic neuron (DAN) clusters and the
546 mushroom body (MB) in the third-instar larval brain. **(b)** & **(c)** Schematic diagrams show the
547 innervation patterns from distinct DANs to different compartments in the MB. All 11 MB
548 compartments are shown, note that there is no synapse formed from dopaminergic neurons to
549 the calyx and intermediate peduncle (IP). DANs in DL1 (b) and in pPAM (c). **(d-m)** Drivers covering
550 DANs in the DL1 cluster (d-h). Drivers covering DANs in the pPAM cluster (i-m). The first column
551 shows drivers covering distinct dopaminergic neurons. Neurons under the drivers are labeled by
552 GFP, the mushroom body (MB) is labeled by RFP, and dopaminergic neurons (DANs) are marked
553 by tyrosine hydroxylase (TH) antibody. The second column (d'-m') shows the GRASP signals from
554 DANs under the driver to the corresponding compartments in the MB. The green channel
555 represents the GRASP signals, and RFP marks the morphology of the MB. In the first column,
556 white arrows mark the DANs under the driver strains. Yellow arrows in (d) show the pPAM
557 neurons not labelled by TH-GAL4 driver strain. The yellow arrowhead in (k) showed the DL1
558 neuron not innervating the MB. Scale bars: 50 µm for the first column, and 20 µm for the second
559 column. ***Abbreviations:*** DL, dorsolateral; DM, dorsomedial; IP, intermediate peduncle; IT
560 intermediate toe; IVL, intermediate vertical lobe; LA, lateral appendix; LP, lower peduncle; LT,
561 lower toe; LVL, lower vertical lobe; pPAM, primary protocerebral anterior medial; SHA, shaft; UT,
562 upper toe; UVL, upper vertical lobe. *(Note) GFP expression patterns in the entire larval CNS by*
563 *GAL4 driver strains used in this study can be found in Figure S1.*
564
565
566 **Figure 2. DAN-c1 is both necessary and sufficient for larval aversive learning. (a-f)** R76F02-
567 AD;R55C10-DBD driver is used as it covers one dopaminergic neuron, DAN-c1, in each brain
568 hemisphere. **(a)** Dendrites and axons of DAN-c1 are labeled by DenMark and sytGFP,
569 correspondingly. **(b-e)** The innervation patterns of DAN-c1. DAN-c1 is labeled with GFP, the MB
570 with RFP, and DANs with TH antibody (blue color). Only one DAN soma is identified (c), axons
571 from DAN-c1 innervate the lower peduncle (LP) of the MB (d), and synapses from DAN-c1 to the
572 LP of the MB are shown by GRASP (e). A schematic diagram (f) shows the innervation patterns of
573 DAN-c1. Modified from Eichler *et al.*[46], and Saumweber *et. al*.[28]. **(g)** A schematic paradigm for
574 larval olfactory learning (top) and two different training paradigms for thermogenetics (bottom).
575 **(h-j)** Blocking dopamine release from DAN-c1 during learning using *shibire*^{ts1} strain under 34°C
576 impairs larval aversive learning. **(k-l)** Activation of DAN-c1 with dTRTPA1 under 34°C induces
577 aversive learning. **QUI,** quinine. **DW,** distill water. **SUC,** sucrose. Data are shown as mean ± SEM.
578 Two-way ANOVA, Dunnett multiple comparisons test, *$p < 0.05$, **$p < 0.01$, ***$p < 0.001$, ****p
579 < 0.0001. For N numbers, see Table S2. Scale bars: 50 µm (a and b), 20 µm (c, d and e).
580
581
582 **Figure 3. D2Rs are expressed in dopaminergic neurons and mushroom body in *Drosophila***
583 **larval brains. (a)** The expression pattern of D2R in a general view. D2R is shown with tagged GFP
584 (D2R-GFP). Magenta represents neuropils marked by nc82 antibody (a'). **(b-g)** D2Rs (presynaptic)

are found in most DANs: DM1a (**b**) and DM1b (**c**), pPAM (**d**), DL1 **(e)**, DL2a **(f)**, and DL2b **(g)** clusters. D2Rs are expressed in parts of DL1 neurons (white arrows in **e**) but not in DL2a neurons (yellow arrow heads in **f**). **(h-i)** D2Rs (postsynaptic) are found in soma of mushroom body (MB) neurons (white arrows in **h**), and MB lobes and peduncles (**i**), but not in calyx (yellow arrow heads in **h**). **(j)** A schematic diagram shows the expression pattern of pre- and postsynaptic D2R in DANs and MB (yellow) in the *Drosophila* larval brain, respectively. Scale bars: 200 µm **(a)**; 50 µm (**b-g**); 20 µm **(h, i)**. ***Abbreviations:*** DL, dorsolateral; DM, dorsomedial; pPAM, primary protocerebral anterior medial.

Figure 4. Presynaptic D2R in DAN-c1 is necessary for larval aversive learning. (a) D2R is expressed in DAN-c1. The expression pattern of D2R is shown with tagged GFP, DAN-c1 is marked by mCherry, and all DANs are marked with TH antibody (blue). **(b-c)** Knockdown of D2R by D2R-miR reduces fluorescent intensities of D2R-tagged GFP (D2R-GFP). The TH-GAL4 driver is used to express mCherry. The intensity of D2R-tagged GFP is reduced in the DM1 cluster (yellow arrowheads in b), which is still intact in pPAM neurons (white arrows in c). **(d)** D2R-GFP fluorescent intensity is quantified by standardizing the values in DM1 with those in the pPAM. Data are shown as mean ± SEM. For the TH-GAL4 group, N=32 from 8 brains; for the TH×D2R-miR group, N=24 from 6 brains. Unpaired t test, ****$p < 0.0001$. Scale bar: 20µm. **(e)** Knockdown of D2R in DAN-c1 by D2R-miR impairs larval aversive learning. **QUI,** quinine. **DW,** distill water. **SUC,** sucrose. Data are shown as mean ± SEM. Two-way ANOVA, Dunnett multiple comparisons test, **$p < 0.01$, ***$p < 0.001$, ****$p < 0.0001$. For N numbers, see Table S3. **(f-i)** D2R knockdown in DAN-c1 does not affect naïve sensory and motor functions. Data are shown as mean ± SEM. One-way ANOVA, Tukey multiple comparisons test. For N numbers, see Table S3. *(Note) Figures S5 and S6 show additional information on naïve sensory and motor functions in larvae related to D2R-miR experiments.*

Figure 5. Over-excitation of DAN-c1 impairs larval aversive learning. (a) A schematic diagram of optogenetic manipulations of neuronal excitability in DAN-c1 during distinct stages in learning. **(b-d)** Activation of DAN-c1 during training impairs larval aversive learning (**b**), while keeps appetitive learning intact (**d**). Unconditioned stimuli used were quinine (b) and sucrose (d). No learning behaviors are observed in the control distilled water (DW) groups (**c**). Third-instar larvae with ChR2 expression in DAN-c1 are used. *ATR,* all-trans-retinal. Data are shown as mean ± SEM. Two-way ANOVA, Dunnett multiple comparisons test, ***$p < 0.001$, ****$p < 0.0001$. For N numbers, see Table S4.

Figure 6. D2R in mushroom body is necessary for both aversive and appetitive learning. (a) Knockdown D2R in mushroom body neurons (MBNs) impairs larval aversive and appetitive learning. **(b-d)** Activation of MBNs during training impairs both larval aversive and appetitive learning. Unconditioned stimuli used were quinine (b) and sucrose (d). No learning behaviors are observed in the control distilled water (DW) groups (**c**). Third-instar larvae with ChR2 expression in MBNs (201Y-GAL4) are used. *ATR,* all-trans-retinal. Data are shown as mean ± SEM. Two-way

629 ANOVA, Dunnett multiple comparisons test, *p < 0.05, **p < 0.01, ***p < 0.001, ****p < 0.0001.
630 For N numbers, see Table S3 and S4.
631
632
633 **Figure 7. Roles of D2Rs in dopaminergic and mushroom body neurons during larval**
634 **olfactory learning. (a)** A schematic diagram shows the roles of D2R in dopaminergic neurons
635 (DAN) and mushroom body neurons (MBN) in larval olfactory associative learning**.** During
636 learning, olfactory stimuli (conditioned stimulus, CS) are received by olfactory sensory neurons
637 (OSN) and transmitted to MBNs (green) via projection neurons (PN). Distinct gustatory stimuli
638 (unconditioned stimulus, US) are received by gustatory sensory neurons (GSN) and transferred
639 to different dopaminergic neurons. Aversive stimuli are sent to DAN-c1 (red) in the DL1 cluster
640 which connects the lower peduncle compartment (LP, square in dash line), while appetitive
641 stimuli are received by pPAM neurons (blue) innervating the medial lobe (ML). D2Rs (yellow
642 square) are expressed in DAN-c1 and pPAM as autoreceptors, regulating dopamine release. Both
643 D2R and dDA1 (magenta circle) are expressed in the MBNs. **(b)** A hypothetical curve showing the
644 relationship between learning ability and cAMP level in the mushroom body. Insufficient cAMP
645 (*rutabaga mutant*) cannot induce learning, while excessive cAMP (*dunce mutant*) also impairs
646 learning. Only the appropriate level of cAMP regulated by the opposing actions of D1R (dDA1)
647 and D2R leads to successful learning in wild type larvae (WT). Knockdown of D2R in DAN-c1
648 causes excessive dopamine release, elevating cAMP and resulting in impaired learning. D2R
649 knockdown in MBNs relieves the inhibition effect of D2R, resulting in excessive intracellular cAMP
650 and learning failure. **(c-d)** Potential molecular mechanisms underlying *Drosophila* olfactory
651 learning in the square region shown in (a). **(d)** During aversive learning, olfactory stimuli induce
652 depolarization of MBNs, which activates voltage-gated calcium channels and induces calcium
653 influx. Gustatory stimuli, such as quinine, activates dopaminergic neurons and elevates dopamine
654 (DA) release. D1 receptor (dDA1) activates adenylyl cyclase (AC) and elevates cAMP via $G\alpha_s$, while
655 D2 receptor (D2R) inhibits AC and suppresses cAMP via $G\alpha_{i/o}$. In *Drosophila*, the coincidence
656 detector *rutabaga* (AC) is activated by the existence of both calcium and $G\alpha_s$, converging the
657 olfactory and gustatory stimuli. cAMP activates the PKA signaling pathway, elevating the
658 neuronal excitability. D1 and D2 receptors can also form heteromeric receptors and activate the
659 PLC-PKC and CaMKII signaling pathways via $G\alpha_q$. These pathways inhibit acetylcholine (ACh)
660 release from MBNs to MB output neurons (MBON), which leads to avoidance of the learned odor.
661 ***Abbreviations:*** AC, adenylyl cyclase; ACh, acetylcholine; ATP, adenosine triphosphate; CaM,
662 calmodulin; CaMKII, Ca^{2+}/calmodulin-dependent protein kinase II; cAMP, cyclic adenosine
663 monophosphate; CS, conditioned stimulus; DA, dopamine; DAN, dopaminergic neurons; DL,
664 dorsolateral; ER, endoplasmic reticulum; $G\alpha_{i/o}$, $G_{i/o}$ protein α subunit; $G\alpha_q$, G_q protein α subunit;
665 $G\alpha_s$, G_s protein α subunit; GSN, gustatory sensory neurons; LP, lower peduncle; MBN, mushroom
666 body neurons; MBON, mushroom body output neurons; ML, medial lobe; nAChR, nicotinic
667 acetylcholine receptor; OSN, olfactory sensory neurons; PKA, protein kinase A; PKC, protein
668 kinase C; PLC, phospholipase C; PN, projection neurons; pPAM, primary protocerebral anterior
669 medial; RyR, ryanodine receptor; US, unconditioned stimulus; VGCC, voltage gated calcium
670 channel.

671 **Table 1. Driver strains screened for dopaminergic neurons in the third-instar larval brain.**
672 Strains are listed with their published names and names used in this work. The numbers of
673 dopaminergic and non-dopaminergic neurons in the third-instar larval brain are described. The
674 identities of dopaminergic neurons from distinct clusters are also listed, especially for those in
675 DL1 and pPAM. The analogs column lists the labelled neurons in previous publications.
676 Source/Gift column shows the original papers in which these strains were described, as well as
677 the laboratories these strains were obtained from. Several, 2-5 neurons; some, 6-10 neurons;
678 lots, >10 neurons.
679

682 **Supplemental information**
683
684 **Figure S1. GFP expression patterns in the larval CNS by GAL4 driver strains used in this study.**
685 **(a-n)** Representative pictures show the patterns of distinct GAL4 driver strains crossed with a
686 UAS-GFP strain. **(o)** A representative picture shows the pattern of MB247-LexA driver (MB247-
687 LexA::VP16) crossed with a LexAop-RFP strain (LexAop-rCD2::RFP). Blue channel represents
688 neuropils marked by nc82 antibody. Driver strains in **(a-j)** were used in **Figure 1d-m.** Driver strains
689 in **(k-m)** are strains used in supplementary **Figure S3**. 201Y-Gal4 (N) is the driver strain used in
690 **Figure 6**. Scale bar: 200 µm.
691
692
693 **Figure S2. Controls for GRASP experiments. (a-c)** The GRASP signals were not observed in
694 control groups. The first column shows the mouse anti-GFP staining (green) for GRASP signals,
695 the second column shows MB lobes by RFP (red), and the third column shows the rabbit anti-GFP
696 staining (blue) which only recognizes the spGFP1-10. **(a)** Both GRASP (mouse antibody, green)
697 and spGFP1-10 (rabbit antibody, blue) can be recognized in the lower peduncle (LP) compartment
698 (white arrows), in a larval brain expressing spGFP1-10 under TH-Gal4 and spGFP11 under MB247-
699 LexA. Some strong spGFP1-10 signals outside of MB are also colocalized with GRASP signals
700 (yellow arrowheads). **(b)** GRASP signals are hardly observed in a larval brain only expressing
701 spGFP1-10 under TH-Gal4 (no MB247-LexA in this brain), while anti-spGFP1-10 signals are still
702 strong (magenta arrows). **(c)** Neither GRASP nor spGFP1-10 can be recognized in a larval brain
703 only expressing spGFP11 under MB247-LexA (cyan arrowheads). Scale bars: 20 µm. **(d)** A
704 Schematic diagram shows the mechanism of GRASP. Modified from Macpherson et. al.[89].
705
706
707 **Figure S3. D2R-GAL4 strains support the expression pattern of D2R. (a-b)** Control staining
708 for D2R-tagged GFP in **Figure 3**. The green channel represents GFP signals whereas magenta
709 represents neuropils marked by nc82 antibody. GFP staining in WT (a). Secondary antibody only
710 staining for the D2R-tagged GFP strain (b). **(c-e)** D2R-GAL4 strains support the expression of D2R
711 in some DANs. The green channel represents GFP signals, red represents mCherry signals under
712 D2R-GAL4 drivers, and blue marks DANs with TH antibodies. R72C08 labels three DM1 neurons
713 (c). R72C04 labels one DM1 (d) and two DL2b neurons (e). **(f-h)** D2R-GAL4 strains support the
714 expression of D2R in mushroom body neurons. The green channel represents GFP signals, and
715 red represents mCherry signals under D2R-GAL4 drivers. R72D03 marks some MBNs in
716 mushroom body (f). R72C08 labels some MBNs in axons (g), dendrites and soma (h). **(i)** D2R is
717 absent in the core of mushroom body lobes, from a transection view of the lower peduncle. Scale
718 bars: 200 µm (**a and b**); 20 µm (**c-e, g-i**), 50 µm (**f**).
719
720
721 **Figure S4. D2Rs in DAN-d1 and DAN-g1 are not necessary for aversive learning. (a-b)**
722 Dendrites and axons of DAN-d1 (a) and g1 (b) are labeled by DenMark (red) and sytGFP (green),
723 correspondingly. **(c-d)** D2Rs are expressed in DAN-d1 (c) and DAN-g1 (d). The expression pattern
724 of D2R is shown with tagged-GFP, DAN-g1 and d1 are marked by mCherry, and DANs are labeled
725 by TH-antibody (blue). **(e)** Knockdown D2R in neither in DAN-g1 nor DAN-d1 impairs aversive

726 learning. Data are shown as mean ± SEM. Two-way ANOVA, Dunnett multiple comparisons test,
727 **p < 0.01, ***p < 0.001, ****p < 0.0001. For N numbers, see Table S3. **(f)** The gene structure of
728 D2R, the insertion site of GFP, and the D2R-microRNA targeting sequence are shown in a
729 schematic diagram. Modified from Xie and Ho[61]. Scale bars: 50 µm (a and b), 20 µm (c and d).
730
731
732 **Figure S5. Knockdown D2R in DAN-c1 with a RNAi strain also impairs aversive learning. (a)**
733 Knockdown of D2R with D2R-miR in DAN-c1 impairs larval aversive learning when using propionic
734 acid as the odorant. **(b)** Knockdown of D2R in DAN-c1 with a RNAi strain also impairs larval
735 aversive learning when using pentyl acetate as the odorant, while knockdown of D2R in either
736 DAN-d1 or g1 does not affect learning. **(c)** Knockdown of D2R with D2R-miR in DANs under TH-
737 GAL4 impairs larval aversive learning when using pentyl acetate as the odorant. Data are shown
738 as mean ± SEM. Two-way ANOVA, Dunnett multiple comparisons test, *p < 0.01, **p < 0.01, ***p
739 < 0.001, ****p < 0.0001. For N numbers, see Table S3.
740
741
742 **Figure S6. Naïve sensory and motor functions of *Drosophila* larvae. (a-e)** The naïve sensory
743 and motor functions in larvae related to D2R-miR experiments. **(a)** No significant difference exists
744 between strains in naïve olfactory tests toward pentyl acetate (PA). **(b)** No significant difference
745 exists between strains in naïve olfactory tests toward propionic acid (ProA). **(c)** No significant
746 difference exists between strains in naïve gustatory tests toward quinine (QUI). **(d)** No significant
747 difference exists between strains in naïve gustatory tests toward sucrose (SUC). **(e)** No significant
748 difference is found between strains and WT, except DAN-c1. So, larvae from DAN-c1 × WT are
749 used for all behavioral assays (refer to **i**). **(f-i)** The naïve sensory and motor functions in larvae
750 related to RNAi experiments. **(f)** No significant difference exists between strains and WT. **(g)** No
751 significant difference exists between strains in naïve gustatory tests toward QUI. **(h)** No
752 significant difference exists between strains in naïve gustatory tests toward SUC. **(i)** There is a
753 significant difference between strains in larval locomotion speed, and there is significant
754 difference between DAN-d1, DAN-d1 × RNAi and WT, but these differences do not affect the
755 learning ability of larvae. Data are shown as mean ± SEM. One-way ANOVA, Tukey multiple
756 comparisons test. For N numbers, see Table S3.
757
758
759 **Figure S7. Over-excitation of DANs during learning impairs larval aversive learning.** Third
760 instar larvae with ChR2 expression in most DANs (TH-Gal4) were used. Activation of DANs during
761 training impairs larval aversive learning (**a**), while keeps appetitive learning intact (**c**). No learning
762 behaviors are observed in the control distilled water (DW) groups **(b)**. Data are shown as mean ±
763 SEM. Two-way ANOVA, Dunnett multiple comparisons test, ***p < 0.001. For N numbers, see
764 Table S4.
765

766 **Supplementary Tables**
767
768 **Table S1. Other strains used in this study.**
769
770 **Table S2. N numbers of learning assays with thermogenetics.**
771
772 **Table S3. N numbers of DD2R knockdown experiments.**
773
774 **Table S4. N numbers of learning assays with optogenetics**
775

776 **Reference:**

777 1 Kandel, E. R., Dudai, Y. & Mayford, M. R. The molecular and systems biology of memory.
778 *Cell* **157**, 163-186 (2014). https://doi.org/10.1016/j.cell.2014.03.001
779 2 Neve, K. A., Seamans, J. K. & Trantham-Davidson, H. Dopamine receptor signaling. *J*
780 *Recept Signal Transduct Res* **24**, 165-205 (2004). https://doi.org/10.1081/rrs-200029981
781 3 Baik, J. H. Dopamine signaling in reward-related behaviors. *Front Neural Circuits* **7**, 152
782 (2013). https://doi.org/10.3389/fncir.2013.00152
783 4 Missale, C., Nash, S. R., Robinson, S. W., Jaber, M. & Caron, M. G. Dopamine receptors:
784 from structure to function. *Physiol Rev* **78**, 189-225 (1998).
785 https://doi.org/10.1152/physrev.1998.78.1.189
786 5 Bjorklund, A. & Dunnett, S. B. Dopamine neuron systems in the brain: an update. *Trends*
787 *Neurosci* **30**, 194-202 (2007). https://doi.org/10.1016/j.tins.2007.03.006
788 6 Puig, M. V., Antzoulatos, E. G. & Miller, E. K. Prefrontal dopamine in associative learning
789 and memory. *Neuroscience* **282**, 217-229 (2014).
790 https://doi.org/10.1016/j.neuroscience.2014.09.026
791 7 Barrot, M. The ventral tegmentum and dopamine: A new wave of diversity.
792 *Neuroscience* **282**, 243-247 (2014). https://doi.org/10.1016/j.neuroscience.2014.10.017
793 8 Savica, R. & Benarroch, E. E. Dopamine receptor signaling in the forebrain: recent
794 insights and clinical implications. *Neurology* **83**, 758-767 (2014).
795 https://doi.org/10.1212/WNL.0000000000000719
796 9 Beaulieu, J. M. & Gainetdinov, R. R. The physiology, signaling, and pharmacology of
797 dopamine receptors. *Pharmacol Rev* **63**, 182-217 (2011).
798 https://doi.org/10.1124/pr.110.002642
799 10 Klein, M. O. *et al.* Dopamine: Functions, Signaling, and Association with Neurological
800 Diseases. *Cell Mol Neurobiol* **39**, 31-59 (2019). https://doi.org/10.1007/s10571-018-
801 0632-3
802 11 Waddell, S. Dopamine reveals neural circuit mechanisms of fly memory. *Trends Neurosci*
803 **33**, 457-464 (2010). https://doi.org/10.1016/j.tins.2010.07.001
804 12 Berry, J., Krause, W. C. & Davis, R. L. Olfactory memory traces in Drosophila. *Prog Brain*
805 *Res* **169**, 293-304 (2008). https://doi.org/10.1016/S0079-6123(07)00018-0
806 13 Bellen, H. J., Tong, C. & Tsuda, H. 100 years of Drosophila research and its impact on
807 vertebrate neuroscience: a history lesson for the future. *Nat Rev Neurosci* **11**, 514-522
808 (2010). https://doi.org/10.1038/nrn2839
809 14 Yamamoto, S. & Seto, E. S. Dopamine dynamics and signaling in Drosophila: an overview
810 of genes, drugs and behavioral paradigms. *Exp Anim* **63**, 107-119 (2014).
811 https://doi.org/10.1538/expanim.63.107
812 15 Heisenberg, M. Mushroom body memoir: from maps to models. *Nat Rev Neurosci* **4**,
813 266-275 (2003). https://doi.org/10.1038/nrn1074
814 16 Davis, R. L. Olfactory learning. *Neuron* **44**, 31-48 (2004).
815 https://doi.org/10.1016/j.neuron.2004.09.008
816 17 Honjo, K. & Furukubo-Tokunaga, K. Induction of cAMP response element-binding
817 protein-dependent medium-term memory by appetitive gustatory reinforcement in
818 Drosophila larvae. *J Neurosci* **25**, 7905-7913 (2005).
819 https://doi.org/10.1523/JNEUROSCI.2135-05.2005

820 18 Honjo, K. & Furukubo-Tokunaga, K. Distinctive neuronal networks and biochemical
821 pathways for appetitive and aversive memory in Drosophila larvae. *J Neurosci* **29**, 852-
822 862 (2009). https://doi.org/10.1523/JNEUROSCI.1315-08.2009
823 19 Widmann, A. *et al.* Genetic Dissection of Aversive Associative Olfactory Learning and
824 Memory in Drosophila Larvae. *PLoS Genet* **12**, e1006378 (2016).
825 https://doi.org/10.1371/journal.pgen.1006378
826 20 Quinn, W. G., Harris, W. A. & Benzer, S. Conditioned behavior in Drosophila
827 melanogaster. *Proc Natl Acad Sci U S A* **71**, 708-712 (1974).
828 https://doi.org/10.1073/pnas.71.3.708
829 21 Tempel, B. L., Bonini, N., Dawson, D. R. & Quinn, W. G. Reward learning in normal and
830 mutant Drosophila. *Proc Natl Acad Sci U S A* **80**, 1482-1486 (1983).
831 https://doi.org/10.1073/pnas.80.5.1482
832 22 Roman, G. & Davis, R. L. Molecular biology and anatomy of Drosophila olfactory
833 associative learning. *Bioessays* **23**, 571-581 (2001). https://doi.org/10.1002/bies.1083
834 23 Quinn, W. G. & Dudai, Y. Memory phases in Drosophila. *Nature* **262**, 576-577 (1976).
835 https://doi.org/10.1038/262576a0
836 24 Waddell, S., Armstrong, J. D., Kitamoto, T., Kaiser, K. & Quinn, W. G. The amnesiac gene
837 product is expressed in two neurons in the Drosophila brain that are critical for memory.
838 *Cell* **103**, 805-813 (2000). https://doi.org/10.1016/s0092-8674(00)00183-5
839 25 Dudai, Y., Jan, Y. N., Byers, D., Quinn, W. G. & Benzer, S. dunce, a mutant of Drosophila
840 deficient in learning. *Proc Natl Acad Sci U S A* **73**, 1684-1688 (1976).
841 https://doi.org/10.1073/pnas.73.5.1684
842 26 Davis, R. L. & Dauwalder, B. The Drosophila dunce locus: learning and memory genes in
843 the fly. *Trends Genet* **7**, 224-229 (1991). https://doi.org/10.1016/0168-9525(91)90369-2
844 27 Crittenden, J. R., Skoulakis, E. M., Han, K. A., Kalderon, D. & Davis, R. L. Tripartite
845 mushroom body architecture revealed by antigenic markers. *Learn Mem* **5**, 38-51
846 (1998).
847 28 Saumweber, T. *et al.* Functional architecture of reward learning in mushroom body
848 extrinsic neurons of larval Drosophila. *Nat Commun* **9**, 1104 (2018).
849 https://doi.org/10.1038/s41467-018-03130-1
850 29 Stocker, R. F. Drosophila as a focus in olfactory research: mapping of olfactory sensilla
851 by fine structure, odor specificity, odorant receptor expression, and central connectivity.
852 *Microsc Res Tech* **55**, 284-296 (2001). https://doi.org/10.1002/jemt.1178
853 30 Ramaekers, A. *et al.* Glomerular maps without cellular redundancy at successive levels
854 of the Drosophila larval olfactory circuit. *Curr Biol* **15**, 982-992 (2005).
855 https://doi.org/10.1016/j.cub.2005.04.032
856 31 Wong, A. M., Wang, J. W. & Axel, R. Spatial representation of the glomerular map in the
857 Drosophila protocerebrum. *Cell* **109**, 229-241 (2002). https://doi.org/10.1016/s0092-
858 8674(02)00707-9
859 32 Lee, T., Lee, A. & Luo, L. Development of the Drosophila mushroom bodies: sequential
860 generation of three distinct types of neurons from a neuroblast. *Development* **126**,
861 4065-4076 (1999). https://doi.org/10.1242/dev.126.18.4065

862 33. Mao, Z. & Davis, R. L. Eight different types of dopaminergic neurons innervate the
863 Drosophila mushroom body neuropil: anatomical and physiological heterogeneity. *Front*
864 *Neural Circuits* **3**, 5 (2009). https://doi.org/10.3389/neuro.04.005.2009
865 34 Blanco, J., Pandey, R., Wasser, M. & Udolph, G. Orthodenticle is necessary for survival of
866 a cluster of clonally related dopaminergic neurons in the Drosophila larval and adult
867 brain. *Neural Dev* **6**, 34 (2011). https://doi.org/10.1186/1749-8104-6-34
868 35 Schroll, C. *et al.* Light-induced activation of distinct modulatory neurons triggers
869 appetitive or aversive learning in Drosophila larvae. *Curr Biol* **16**, 1741-1747 (2006).
870 https://doi.org/10.1016/j.cub.2006.07.023
871 36 Sugamori, K. S., Demchyshyn, L. L., McConkey, F., Forte, M. A. & Niznik, H. B. A
872 primordial dopamine D1-like adenylyl cyclase-linked receptor from Drosophila
873 melanogaster displaying poor affinity for benzazepines. *FEBS Lett* **362**, 131-138 (1995).
874 https://doi.org/10.1016/0014-5793(95)00224-w
875 37 Han, K. A., Millar, N. S., Grotewiel, M. S. & Davis, R. L. DAMB, a novel dopamine receptor
876 expressed specifically in Drosophila mushroom bodies. *Neuron* **16**, 1127-1135 (1996).
877 https://doi.org/10.1016/s0896-6273(00)80139-7
878 38 Hearn, M. G. *et al.* A Drosophila dopamine 2-like receptor: Molecular characterization
879 and identification of multiple alternatively spliced variants. *Proc Natl Acad Sci U S A* **99**,
880 14554-14559 (2002). https://doi.org/10.1073/pnas.202498299
881 39 Srivastava, D. P. *et al.* Rapid, nongenomic responses to ecdysteroids and catecholamines
882 mediated by a novel Drosophila G-protein-coupled receptor. *J Neurosci* **25**, 6145-6155
883 (2005). https://doi.org/10.1523/JNEUROSCI.1005-05.2005
884 40 Kim, Y. C., Lee, H. G., Seong, C. S. & Han, K. A. Expression of a D1 dopamine receptor
885 dDA1/DmDOP1 in the central nervous system of Drosophila melanogaster. *Gene Expr*
886 *Patterns* **3**, 237-245 (2003). https://doi.org/10.1016/s1567-133x(02)00098-4
887 41 Selcho, M., Pauls, D., Han, K. A., Stocker, R. F. & Thum, A. S. The role of dopamine in
888 Drosophila larval classical olfactory conditioning. *PLoS One* **4**, e5897 (2009).
889 https://doi.org/10.1371/journal.pone.0005897
890 42 Kim, Y. C., Lee, H. G. & Han, K. A. D1 dopamine receptor dDA1 is required in the
891 mushroom body neurons for aversive and appetitive learning in Drosophila. *J Neurosci*
892 **27**, 7640-7647 (2007). https://doi.org/10.1523/JNEUROSCI.1167-07.2007
893 43 Scholz-Kornehl, S. & Schwarzel, M. Circuit Analysis of a Drosophila Dopamine Type 2
894 Receptor That Supports Anesthesia-Resistant Memory. *J Neurosci* **36**, 7936-7945 (2016).
895 https://doi.org/10.1523/JNEUROSCI.4475-15.2016
896 44 Zhou, M. *et al.* Suppression of GABAergic neurons through D2-like receptor secures
897 efficient conditioning in Drosophila aversive olfactory learning. *Proc Natl Acad Sci U S A*
898 **116**, 5118-5125 (2019). https://doi.org/10.1073/pnas.1812342116
899 45 Draper, I., Kurshan, P. T., McBride, E., Jackson, F. R. & Kopin, A. S. Locomotor activity is
900 regulated by D2-like receptors in Drosophila: an anatomic and functional analysis. *Dev*
901 *Neurobiol* **67**, 378-393 (2007). https://doi.org/10.1002/dneu.20355
902 46 Eichler, K. *et al.* The complete connectome of a learning and memory centre in an insect
903 brain. *Nature* **548**, 175-182 (2017). https://doi.org/10.1038/nature23455
904 47 Tanaka, N. K., Tanimoto, H. & Ito, K. Neuronal assemblies of the Drosophila mushroom
905 body. *J Comp Neurol* **508**, 711-755 (2008). https://doi.org/10.1002/cne.21692

48 Kunz, T., Kraft, K. F., Technau, G. M. & Urbach, R. Origin of Drosophila mushroom body neuroblasts and generation of divergent embryonic lineages. *Development* **139**, 2510-2522 (2012). https://doi.org/10.1242/dev.077883

49 Kurusu, M. *et al.* Embryonic and larval development of the Drosophila mushroom bodies: concentric layer subdivisions and the role of fasciclin II. *Development* **129**, 409-419 (2002). https://doi.org/10.1242/dev.129.2.409

50 Rohwedder, A. *et al.* Four Individually Identified Paired Dopamine Neurons Signal Reward in Larval Drosophila. *Curr Biol* **26**, 661-669 (2016). https://doi.org/10.1016/j.cub.2016.01.012

51 Friggi-Grelin, F. *et al.* Targeted gene expression in Drosophila dopaminergic cells using regulatory sequences from tyrosine hydroxylase. *J Neurobiol* **54**, 618-627 (2003). https://doi.org/10.1002/neu.10185

52 Busto, G. U., Cervantes-Sandoval, I. & Davis, R. L. Olfactory learning in Drosophila. *Physiology (Bethesda)* **25**, 338-346 (2010). https://doi.org/10.1152/physiol.00026.2010

53 Waddell, S. Reinforcement signalling in Drosophila; dopamine does it all after all. *Curr Opin Neurobiol* **23**, 324-329 (2013). https://doi.org/10.1016/j.conb.2013.01.005

54 Aso, Y. & Rubin, G. M. Dopaminergic neurons write and update memories with cell-type-specific rules. *Elife* **5** (2016). https://doi.org/10.7554/eLife.16135

55 Schwaerzel, M. *et al.* Dopamine and octopamine differentiate between aversive and appetitive olfactory memories in Drosophila. *J Neurosci* **23**, 10495-10502 (2003). https://doi.org/10.1523/JNEUROSCI.23-33-10495.2003

56 Aso, Y. *et al.* Three dopamine pathways induce aversive odor memories with different stability. *PLoS Genet* **8**, e1002768 (2012). https://doi.org/10.1371/journal.pgen.1002768

57 Masek, P., Worden, K., Aso, Y., Rubin, G. M. & Keene, A. C. A dopamine-modulated neural circuit regulating aversive taste memory in Drosophila. *Curr Biol* **25**, 1535-1541 (2015). https://doi.org/10.1016/j.cub.2015.04.027

58 Liu, C. *et al.* A subset of dopamine neurons signals reward for odour memory in Drosophila. *Nature* **488**, 512-516 (2012). https://doi.org/10.1038/nature11304

59 Burke, C. J. *et al.* Layered reward signalling through octopamine and dopamine in Drosophila. *Nature* **492**, 433-437 (2012). https://doi.org/10.1038/nature11614

60 Yamagata, N. *et al.* Distinct dopamine neurons mediate reward signals for short- and long-term memories. *Proc Natl Acad Sci U S A* **112**, 578-583 (2015). https://doi.org/10.1073/pnas.1421930112

61 Xie, T. *et al.* A Genetic Toolkit for Dissecting Dopamine Circuit Function in Drosophila. *Cell Rep* **23**, 652-665 (2018). https://doi.org/10.1016/j.celrep.2018.03.068

62 Aso, Y. *et al.* Specific dopaminergic neurons for the formation of labile aversive memory. *Curr Biol* **20**, 1445-1451 (2010). https://doi.org/10.1016/j.cub.2010.06.048

63 Qi, C. & Lee, D. Pre- and Postsynaptic Role of Dopamine D2 Receptor DD2R in Drosophila Olfactory Associative Learning. *Biology (Basel)* **3**, 831-845 (2014). https://doi.org/10.3390/biology3040831

64 Honjo, K., Hwang, R. Y. & Tracey, W. D., Jr. Optogenetic manipulation of neural circuits and behavior in Drosophila larvae. *Nat Protoc* **7**, 1470-1478 (2012). https://doi.org/10.1038/nprot.2012.079

949 65 Boyden, E. S., Zhang, F., Bamberg, E., Nagel, G. & Deisseroth, K. Millisecond-timescale,
950 genetically targeted optical control of neural activity. *Nat Neurosci* **8**, 1263-1268 (2005).
951 https://doi.org/10.1038/nn1525
952 66 Cognigni, P., Felsenberg, J. & Waddell, S. Do the right thing: neural network mechanisms
953 of memory formation, expression and update in Drosophila. *Curr Opin Neurobiol* **49**, 51-
954 58 (2018). https://doi.org/10.1016/j.conb.2017.12.002
955 67 Owald, D. & Waddell, S. Olfactory learning skews mushroom body output pathways to
956 steer behavioral choice in Drosophila. *Curr Opin Neurobiol* **35**, 178-184 (2015).
957 https://doi.org/10.1016/j.conb.2015.10.002
958 68 Davis, R. L. Olfactory memory formation in Drosophila: from molecular to systems
959 neuroscience. *Annu Rev Neurosci* **28**, 275-302 (2005).
960 https://doi.org/10.1146/annurev.neuro.28.061604.135651
961 69 Aso, Y. *et al.* The neuronal architecture of the mushroom body provides a logic for
962 associative learning. *Elife* **3**, e04577 (2014). https://doi.org/10.7554/eLife.04577
963 70 Jefferis, G. S., Marin, E. C., Watts, R. J. & Luo, L. Development of neuronal connectivity in
964 Drosophila antennal lobes and mushroom bodies. *Curr Opin Neurobiol* **12**, 80-86 (2002).
965 https://doi.org/10.1016/s0959-4388(02)00293-3
966 71 Heisenberg, M., Borst, A., Wagner, S. & Byers, D. Drosophila mushroom body mutants
967 are deficient in olfactory learning. *J Neurogenet* **2**, 1-30 (1985).
968 https://doi.org/10.3109/01677068509100140
969 72 de Belle, J. S. & Heisenberg, M. Associative odor learning in Drosophila abolished by
970 chemical ablation of mushroom bodies. *Science* **263**, 692-695 (1994).
971 https://doi.org/10.1126/science.8303280
972 73 Davis, R. L. Traces of Drosophila memory. *Neuron* **70**, 8-19 (2011).
973 https://doi.org/10.1016/j.neuron.2011.03.012
974 74 Sejourne, J. *et al.* Mushroom body efferent neurons responsible for aversive olfactory
975 memory retrieval in Drosophila. *Nat Neurosci* **14**, 903-910 (2011).
976 https://doi.org/10.1038/nn.2846
977 75 Owald, D. *et al.* Activity of defined mushroom body output neurons underlies learned
978 olfactory behavior in Drosophila. *Neuron* **86**, 417-427 (2015).
979 https://doi.org/10.1016/j.neuron.2015.03.025
980 76 Zars, T., Fischer, M., Schulz, R. & Heisenberg, M. Localization of a short-term memory in
981 Drosophila. *Science* **288**, 672-675 (2000). https://doi.org/10.1126/science.288.5466.672
982 77 Tomchik, S. M. & Davis, R. L. Dynamics of learning-related cAMP signaling and stimulus
983 integration in the Drosophila olfactory pathway. *Neuron* **64**, 510-521 (2009).
984 https://doi.org/10.1016/j.neuron.2009.09.029
985 78 Levin, L. R. *et al.* The Drosophila learning and memory gene rutabaga encodes a
986 Ca2+/Calmodulin-responsive adenylyl cyclase. *Cell* **68**, 479-489 (1992).
987 https://doi.org/10.1016/0092-8674(92)90185-f
988 79 Boto, T., Louis, T., Jindachomthong, K., Jalink, K. & Tomchik, S. M. Dopaminergic
989 modulation of cAMP drives nonlinear plasticity across the Drosophila mushroom body
990 lobes. *Curr Biol* **24**, 822-831 (2014). https://doi.org/10.1016/j.cub.2014.03.021

80 Aso, Y. *et al.* Mushroom body output neurons encode valence and guide memory-based action selection in Drosophila. *Elife* **3**, e04580 (2014). https://doi.org/10.7554/eLife.04580

81 Hartenstein, V., Cruz, L., Lovick, J. K. & Guo, M. Developmental analysis of the dopamine-containing neurons of the Drosophila brain. *J Comp Neurol* **525**, 363-379 (2017). https://doi.org/10.1002/cne.24069

82 Tully, T., Cambiazo, V. & Kruse, L. Memory through metamorphosis in normal and mutant Drosophila. *J Neurosci* **14**, 68-74 (1994). https://doi.org/10.1523/JNEUROSCI.14-01-00068.1994

83 Barnstedt, O. *et al.* Memory-Relevant Mushroom Body Output Synapses Are Cholinergic. *Neuron* **89**, 1237-1247 (2016). https://doi.org/10.1016/j.neuron.2016.02.015

84 Wang, Z. W. Regulation of synaptic transmission by presynaptic CaMKII and BK channels. *Mol Neurobiol* **38**, 153-166 (2008). https://doi.org/10.1007/s12035-008-8039-7

85 Eschbach, C. *et al.* Recurrent architecture for adaptive regulation of learning in the insect brain. *Nat Neurosci* **23**, 544-555 (2020). https://doi.org/10.1038/s41593-020-0607-9

86 Winding, M. *et al.* The connectome of an insect brain. *Science* **379**, eadd9330 (2023). https://doi.org/10.1126/science.add9330

87 Nagarkar-Jaiswal, S. *et al.* A genetic toolkit for tagging intronic MiMIC containing genes. *Elife* **4** (2015). https://doi.org/10.7554/eLife.08469

88 Nagarkar-Jaiswal, S. *et al.* A library of MiMICs allows tagging of genes and reversible, spatial and temporal knockdown of proteins in Drosophila. *Elife* **4** (2015). https://doi.org/10.7554/eLife.05338

89 Macpherson, L. J. *et al.* Dynamic labelling of neural connections in multiple colours by trans-synaptic fluorescence complementation. *Nat Commun* **6**, 10024 (2015). https://doi.org/10.1038/ncomms10024

90 Lilly, M. & Carlson, J. smellblind: a gene required for Drosophila olfaction. *Genetics* **124**, 293-302 (1990). https://doi.org/10.1093/genetics/124.2.293

91 Varga, S. J., Qi, C., Podolsky, E. & Lee, D. A new Drosophila model to study the interaction between genetic and environmental factors in Parkinson's disease. *Brain Res* **1583**, 277-286 (2014). https://doi.org/10.1016/j.brainres.2014.08.021

92 Qi, C., Varga, S., Oh, S. J., Lee, C. J. & Lee, D. Optogenetic Rescue of Locomotor Dysfunction and Dopaminergic Degeneration Caused by Alpha-Synuclein and EKO Genes. *Exp Neurobiol* **26**, 97-103 (2017). https://doi.org/10.5607/en.2017.26.2.97

93 Xiao, N., Privman, E. & Venton, B. J. Optogenetic control of serotonin and dopamine release in Drosophila larvae. *ACS Chem Neurosci* **5**, 666-673 (2014). https://doi.org/10.1021/cn500044b

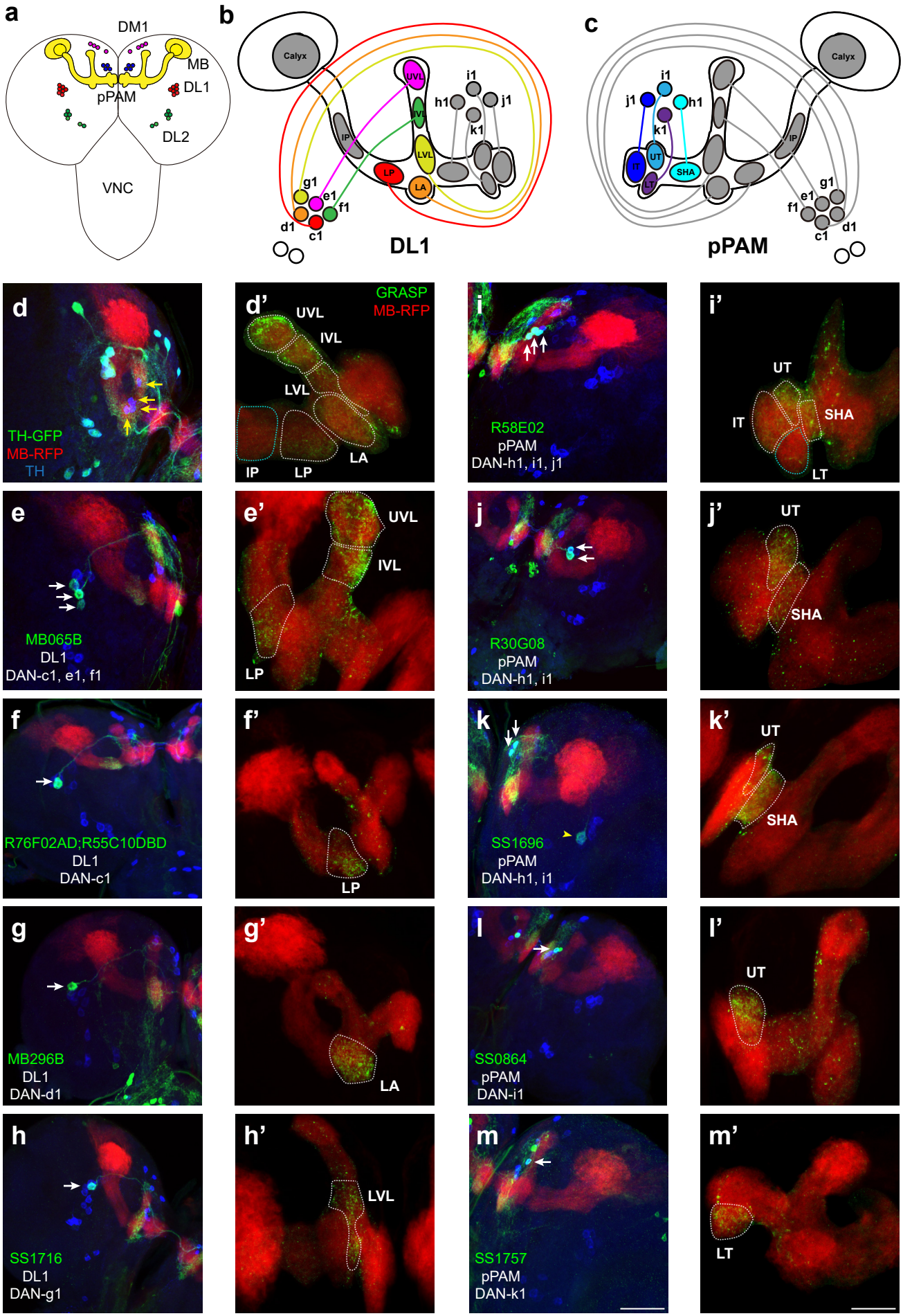
a
DM1
MB
pPAM
DL1
DL2
VNC
b
Calyx
UVL
IVL
LVL
LP
LA
IP
i1
h1
j1
k1
g1
e1
f1
d1
c1
DL1
c
Calyx
i1
j1
h1
k1
IT
UT
LT
SHA
IP
g1
e1
f1
c1
d1
pPAM
d
TH-GFP
MB-RFP
TH
d'
GRASP
MB-RFP
UVL
IVL
LVL
LA
IP
LP
i
R58E02
pPAM
DAN-h1, i1, j1
i'
UT
IT
SHA
LT
e
MB065B
DL1
DAN-c1, e1, f1
e'
UVL
IVL
LP
j
R30G08
pPAM
DAN-h1, i1
j'
UT
SHA
f
R76F02AD;R55C10DBD
DL1
DAN-c1
f'
LP
k
SS1696
pPAM
DAN-h1, i1
k'
UT
SHA
g
MB296B
DL1
DAN-d1
g'
LA
l
SS0864
pPAM
DAN-i1
l'
UT
h
SS1716
DL1
DAN-g1
h'
LVL
m
SS1757
pPAM
DAN-k1
m'
LT

Figure 1

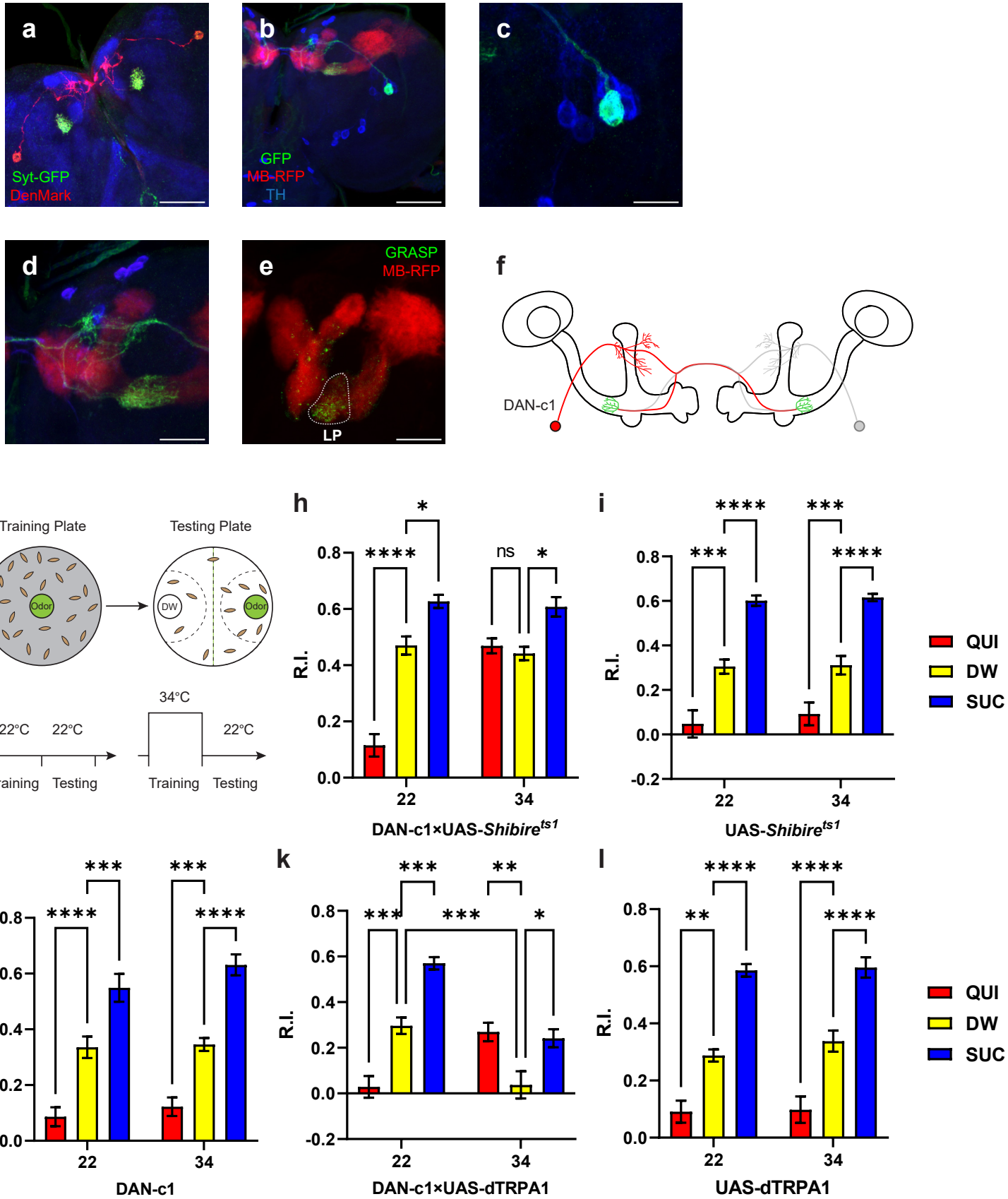
a
Syt-GFP
DenMark
b
GFP
MB-RFP
TH
c
d
e
GRASP
MB-RFP
LP
f
DAN-c1
g
Training Plate
Testing Plate
Odor
DW
Odor
34°C
22°C
22°C
22°C
Training
Testing
Training
Testing
h
R.I.
22
34
DAN-c1×UAS-Shibire^{ts1}
ns
i
UAS-Shibire^{ts1}
QUI
DW
SUC
j
DAN-c1
k
DAN-c1×UAS-dTRPA1
l
UAS-dTRPA1

Figure 2

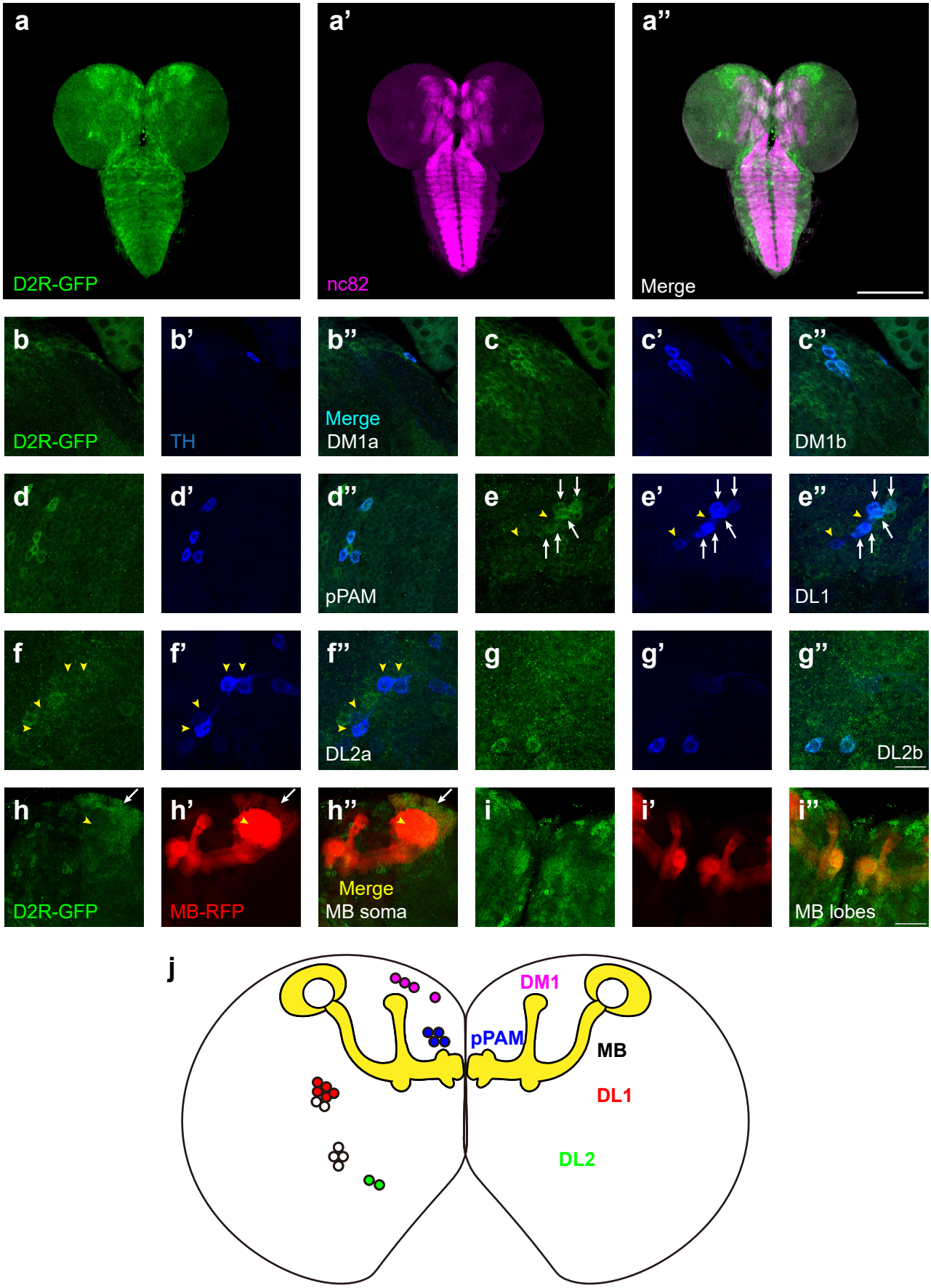
a
D2R-GFP
a'
nc82
a''
Merge
b
D2R-GFP
b'
TH
b''
Merge
DM1a
c
c'
c''
DM1b
d
d'
d''
pPAM
e
e'
e''
DL1
f
f'
f''
DL2a
g
g'
g''
DL2b
h
D2R-GFP
h'
MB-RFP
h''
Merge
MB soma
i
i'
i''
MB lobes
j
DM1
pPAM
MB
DL1
DL2

Figure 3

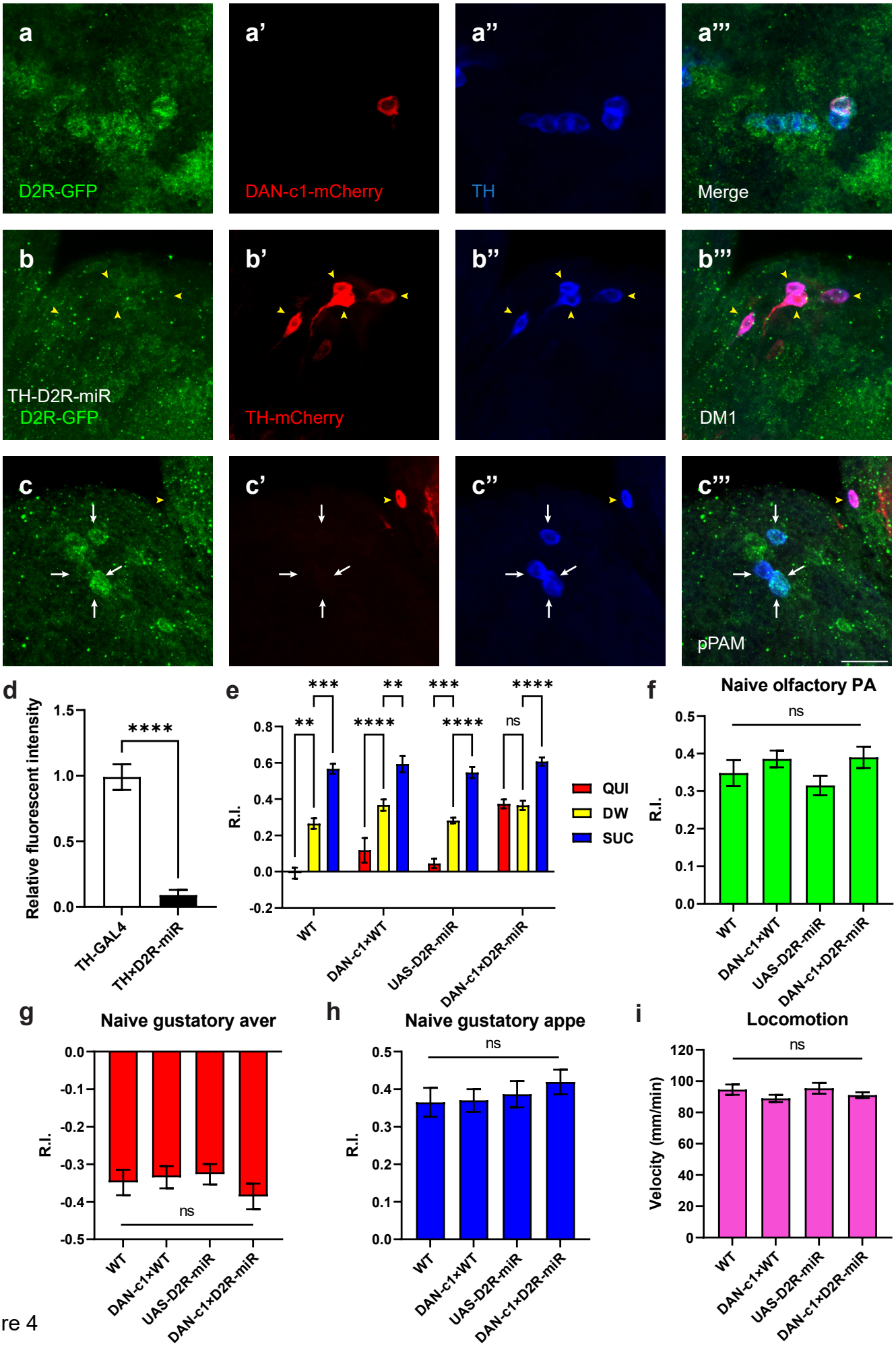
a
D2R-GFP
a'
DAN-c1-mCherry
a''
TH
a'''
Merge
b
TH-D2R-miR
D2R-GFP
b'
TH-mCherry
b''
b'''
DM1
c
c'
c''
c'''
pPAM
d
Relative fluorescent intensity
****
TH-GAL4
TH×D2R-miR
e
R.I.
QUI
DW
SUC
WT
DAN-c1×WT
UAS-D2R-miR
DAN-c1×D2R-miR
f
Naive olfactory PA
ns
g
Naive gustatory aver
h
Naive gustatory appe
i
Locomotion
Velocity (mm/min)

Figure 4

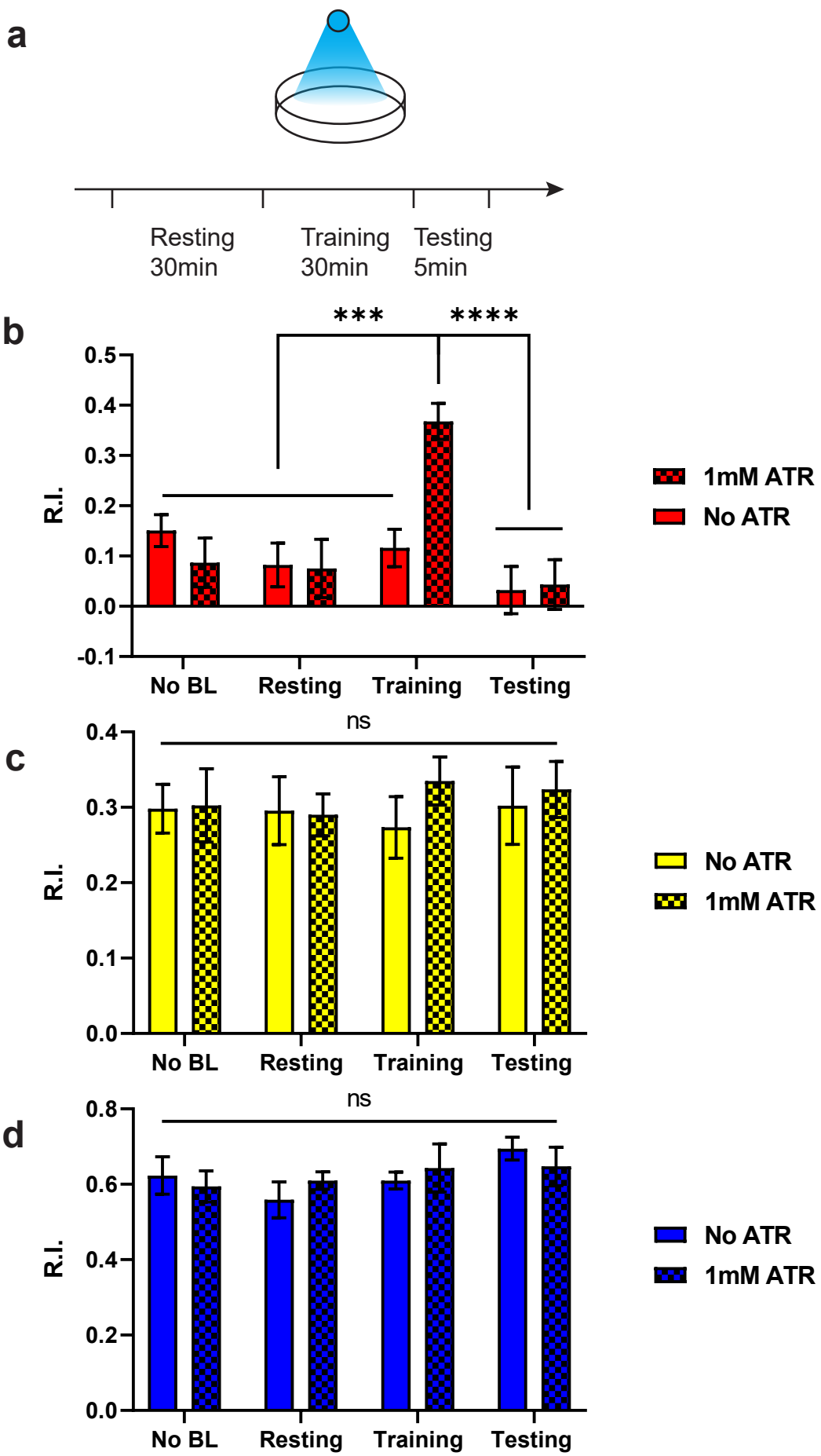
a
Resting
30min
Training
30min
Testing
5min
b
***
****
0.5
0.4
0.3
0.2
0.1
0.0
-0.1
R.I.
No BL
Resting
Training
Testing
1mM ATR
No ATR
c
ns
0.4
0.3
0.2
0.1
0.0
R.I.
No BL
Resting
Training
Testing
No ATR
1mM ATR
d
ns
0.8
0.6
0.4
0.2
0.0
R.I.
No BL
Resting
Training
Testing
No ATR
1mM ATR

Figure 5

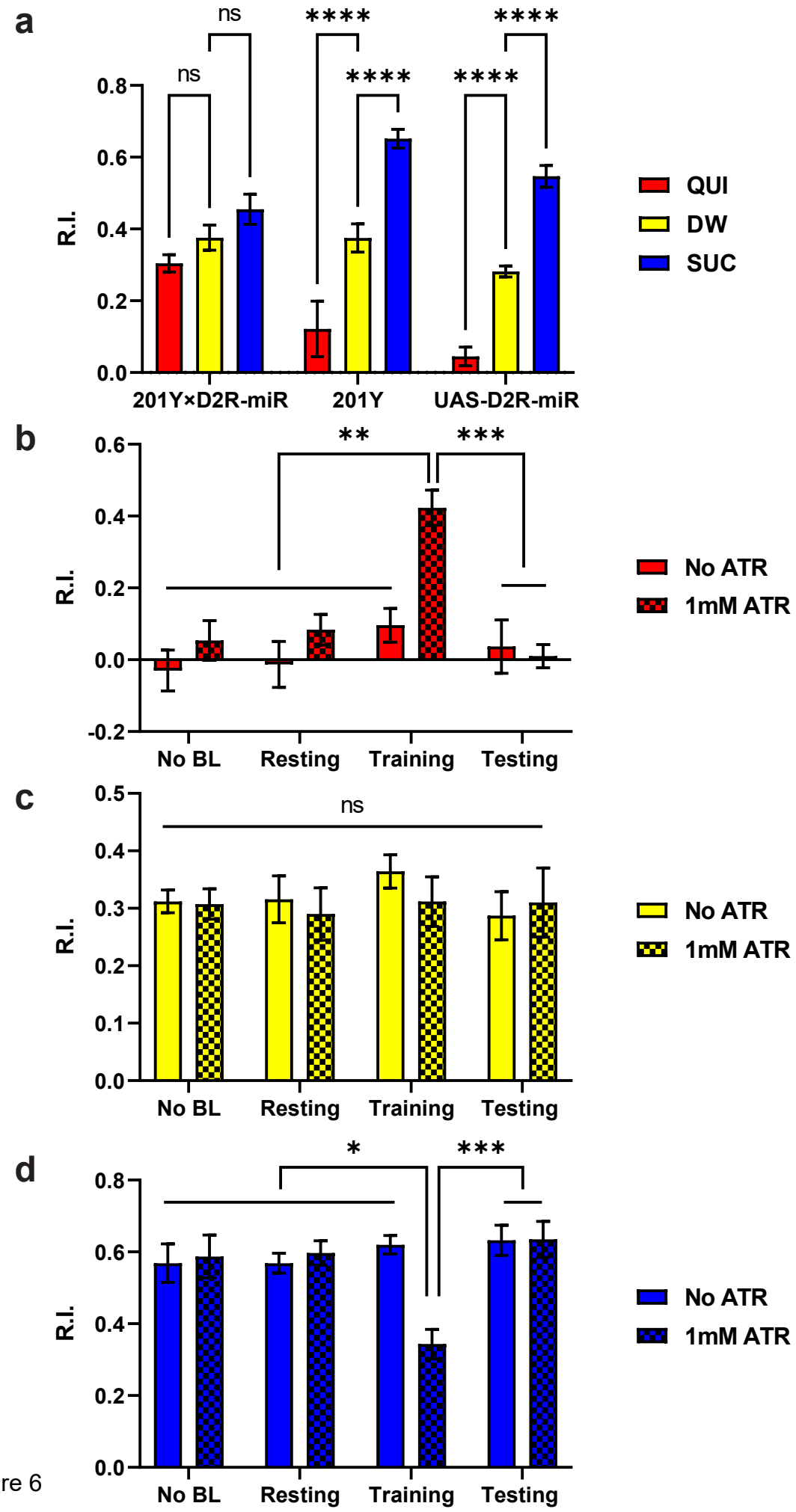
a
ns
ns
****
****
****
****
0.8
0.6
0.4
0.2
0.0
R.I.
201Y×D2R-miR
201Y
UAS-D2R-miR
QUI
DW
SUC
b
**
***
0.6
0.4
0.2
0.0
-0.2
R.I.
No BL
Resting
Training
Testing
No ATR
1mM ATR
c
ns
0.5
0.4
0.3
0.2
0.1
0.0
R.I.
No BL
Resting
Training
Testing
No ATR
1mM ATR
d
*
***
0.8
0.6
0.4
0.2
0.0
R.I.
No BL
Resting
Training
Testing
No ATR
1mM ATR

Figure 6

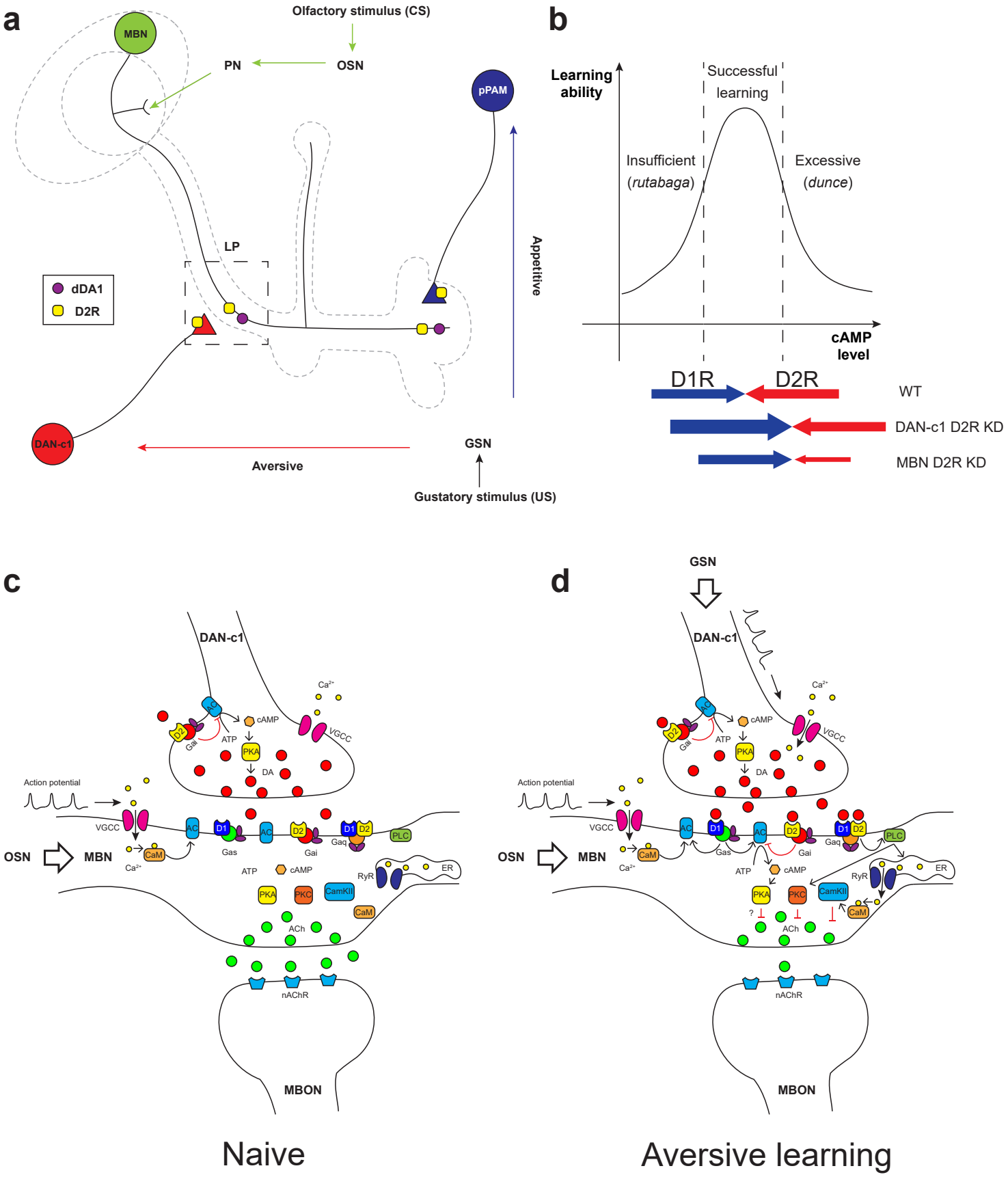
a
Olfactory stimulus (CS)
MBN
PN
OSN
pPAM
LP
dDA1
D2R
Appetitive
DAN-c1
Aversive
GSN
Gustatory stimulus (US)
b
Learning ability
Successful learning
Insufficient (rutabaga)
Excessive (dunce)
cAMP level
D1R
D2R
WT
DAN-c1 D2R KD
MBN D2R KD
c
DAN-c1
Action potential
OSN
MBN
MBON
Naive
d
GSN
DAN-c1
Action potential
OSN
MBN
MBON
Aversive learning

Figure 7

Table 1

	Strains	Name in this work	Neurons in third-instar larval brains		Analogs	Stock #	Source/Gift
			DANs	Non-DANs			
1	TH-Gal4	-	All DANs except pPAM	Some weak	All DANs except PAM (Adult)	-	Dr. J. Hirsh's Lab
2	TH-C'	-	1 DL1, 1 DM1, 3DL2a	Rare	PPL1 + PPM3 (Adult)	-	Dr. M. Wu's lab (Liu et al., 2012)
3	TH-C1	-	-	-	PPL1 + PPM3 (Adult)	-	
4	TH-D'	-	3DL1, 2DL2b	Rare	PPL1 + PPM3 (Adult)	-	
5	TH-D1	-	-	-	PPL1 + PPM3 (Adult)	-	
6	TH-D4	-	-	-	PPL1 + PPM3 (Adult)	-	
7	TH-F1	-	3DL1	Rare	PPL1 + PPM3 (Adult)	-	
8	Th-F2	-	3 DM1, 2-4 DL1, 2DL2a	-	PPL1 + PPM3 (Adult)	-	
9	Th-F3	-	3 DM1b, 1 DL1	-	PPL1 + PPM3 (Adult)	-	
10	TH-G1	-	2-3 DM1, 2-4 DL1, 2 DL2b	-	PPL1 + PPM3 (Adult)	-	
11	R30G08	-	h1, i1, weak k1	-	2 pPAM (L3)	48101	BDSC (Rohwedder et al., 2016)
12	R58E02	-	h1, i1, j1	1	3 pPAM (L3)	41347	
13	R64H06	-	h1, i1, j1, k1	Lots	4 pPAM (L3)	49608	
14	MB315C	-	1-3 pPAM (h1)	Lots	PAM-γ5 (Adult)	-	Janelia Farm (Aso et al., 2014)
15	MB109B	-	-	-	PAM-β'2a (Adult)	-	

16	MB301B	-	-	-	PAM-β2β'2a (Adult)	-	
17	MB056B	-	-	-	PAM-β'2p (Adult)	-	
18	MB032B	-	-	-	PAM-β'2m (Adult)	-	
19	MB312B	-	-	-	PAM-γ4/<γ1γ2 (Adult)	-	
20	MB194B	-	-	-	PAM-β1ped (Adult)	-	
21	MB063B	-	-	-	PAM-β1 (Adult)	-	
22	MB043B	-	h1, i1, j1	Weak, lots of MBN	PAM-α1 (Adult)	-	
23	MB441B	-	-	-	PAM-γ3 (Adult)	-	
24	MB025B	-	-	-	PAM-β'1ap/m (Adult)	-	
25	MB438B	-	-	-	PPL1-γ1pedc (Adult)	-	
26	MB296B	DAN-d1	d1	Some in VNC	PPL1-γ2α'1 (Adult)	-	
27	MB304	-	-	-	PPL1-α'3 (Adult)	-	
28	MB058B	-	-	-	PPL1-α'2α'2 (Adult)	-	
29	MB065B	-	c1, f1, e1	-	PPL1-α3 (Adult)	-	
30	GMR_SS01716	DAN-g1	g1	-	g1 (LVL) (L3)	-	Dr. M. Zlatic's Lab (Saumerber et al., 2018)
31	GMR_SS01696	DAN-h1	h1 + i1	-	h1 (SHA) (L3)	-	
32	GMR_SS00864	DAN-i1	i1	1	i1 (UT) (L3)	-	
33	GMR_SS1757	DAN-k1	k1	1	k1 (LT) (L3)	-	
34	R78E04	-	1 weak DL1	Several	d1 (LA) (L3)	39997	
35	R72B05	-	1 DL1	Lots	MBIN-e2 (L3)	39611	
36	R12C11	-	2 DM1b	Several	MBON-c2 (L3)	76324	
37	R30F04	-	weak d1	Rare	d1 (LA) (L3)	48614	

38	R76C04	-	c1, d1	Rare	c1 (LP) (L3)	48621	
39	R37D06	-	-	-	f1 (IVL) (L3)	47921	
40	R14E06	-	2 DL1	Several	MBIN-e2 (L3)	48643	
41	TH-C-AD;R76F05-DBD	-	1 weak DL1, 2 strong DM1	Lots	PPL1 (SMP-PED) (Adult)	-	Dr. M. Wu's Lab (Xie et al., 2018)
42	TH-F-AD;R61H03-DBD		2DL2, 3 DM1	Rare	PPL1 (SMP) (Adult)	-	
43	R76F02-AD;TH-F-DBD	-	c1, e1	Lots weak	PPL1 (MB-MP1) (Adult)	-	
44	TH-F-AD;R76F05-DBD	-	1 weak DL1, 1-2 strong DM1	Several	PPL1 (SMP-γ) (Adult)	-	
45	R76F02-AD;R60F07-DBD	-	c1, f1, e1	Rare	PPL1 (PED, MB-MP1) (Adult)	-	
46	R60F07-AD;R76F05-DBD	-	g1, e1	Strong SOG	PPL1 (SMP-γ) (Adult)	-	
47	DAT-B-AD;R76F05-DBD	-	2-3pPAM, 1 DL1	Rare	PPL1 (hSMP-γ) (Adult)	-	
48	R76F02-AD;R55C10-DBD	DAN-c1	c1	-	PPL1 (MB-MP1) (Adult)	-	
49	R76F02-AD;R76F01-DBD	-	1 weak DL1	Lots	PPL1 (dFB) (Adult)	-	
50	R76F02-AD;R76F05-DBD	-	-	Lots	PPL1 (dFB) (Adult)	-	
51	R76F05-AD;R61H03-DBD	-	1 DL1, 2 pPAM, 3 DM1	1	PPL1 (MB-MV1) (Adult)	-	
52	WED-1	-	-	-	WED (Adult)	-	Dr. M. Wu's Lab (Liu et al., 2017)
53	WED-2	-	-	-	WED (Adult)	-	
54	TH-FLP/UAS-FRT>>FRT-CD8::GFP;R39G05	-	-	-	PPL1 (bSMP-γ) (Adult)	50063	
55	TH-FLP/UAS-FRT>>FRT-CD8::GFP;R17C11	-	-	-	PPL1 (V1 & MP1) (Adult)	48763	
56	TH-FLP/UAS-FRT>>FRT-CD8::GFP;R39C07	-	2 DL1	-	PPL1 (MV1 & MP1) (Adult)	50039	

57	TH-FLP/UAS-FRT>>FRT-CD8::GFP;R67E08	-	-	-	PPL1 (V1) (Adult)	39445	

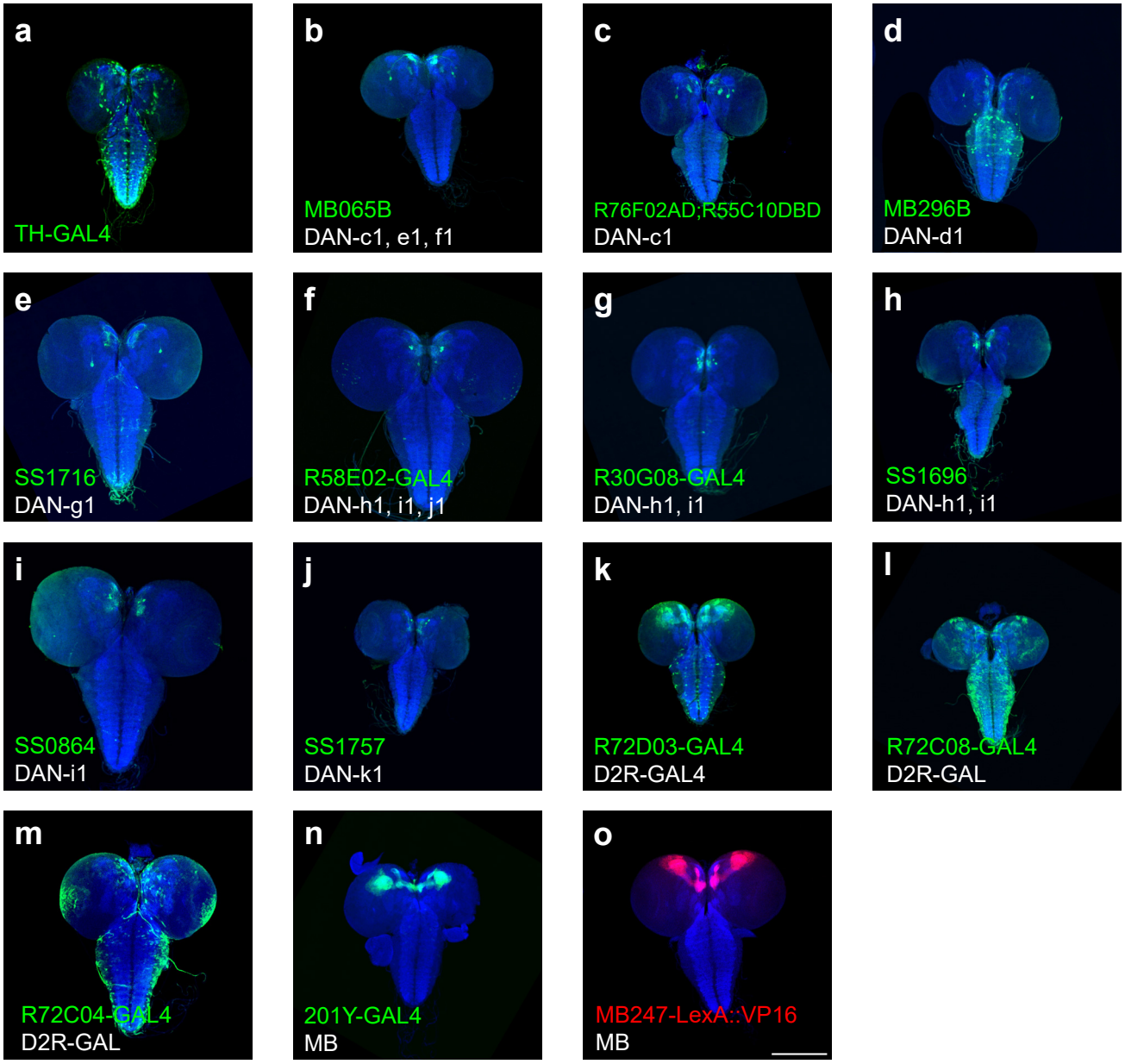
a
TH-GAL4
b
MB065B
DAN-c1, e1, f1
c
R76F02AD;R55C10DBD
DAN-c1
d
MB296B
DAN-d1
e
SS1716
DAN-g1
f
R58E02-GAL4
DAN-h1, i1, j1
g
R30G08-GAL4
DAN-h1, i1
h
SS1696
DAN-h1, i1
i
SS0864
DAN-i1
j
SS1757
DAN-k1
k
R72D03-GAL4
D2R-GAL4
l
R72C08-GAL4
D2R-GAL
m
R72C04-GAL4
D2R-GAL
n
201Y-GAL4
MB
o
MB247-LexA::VP16
MB

Figure S1

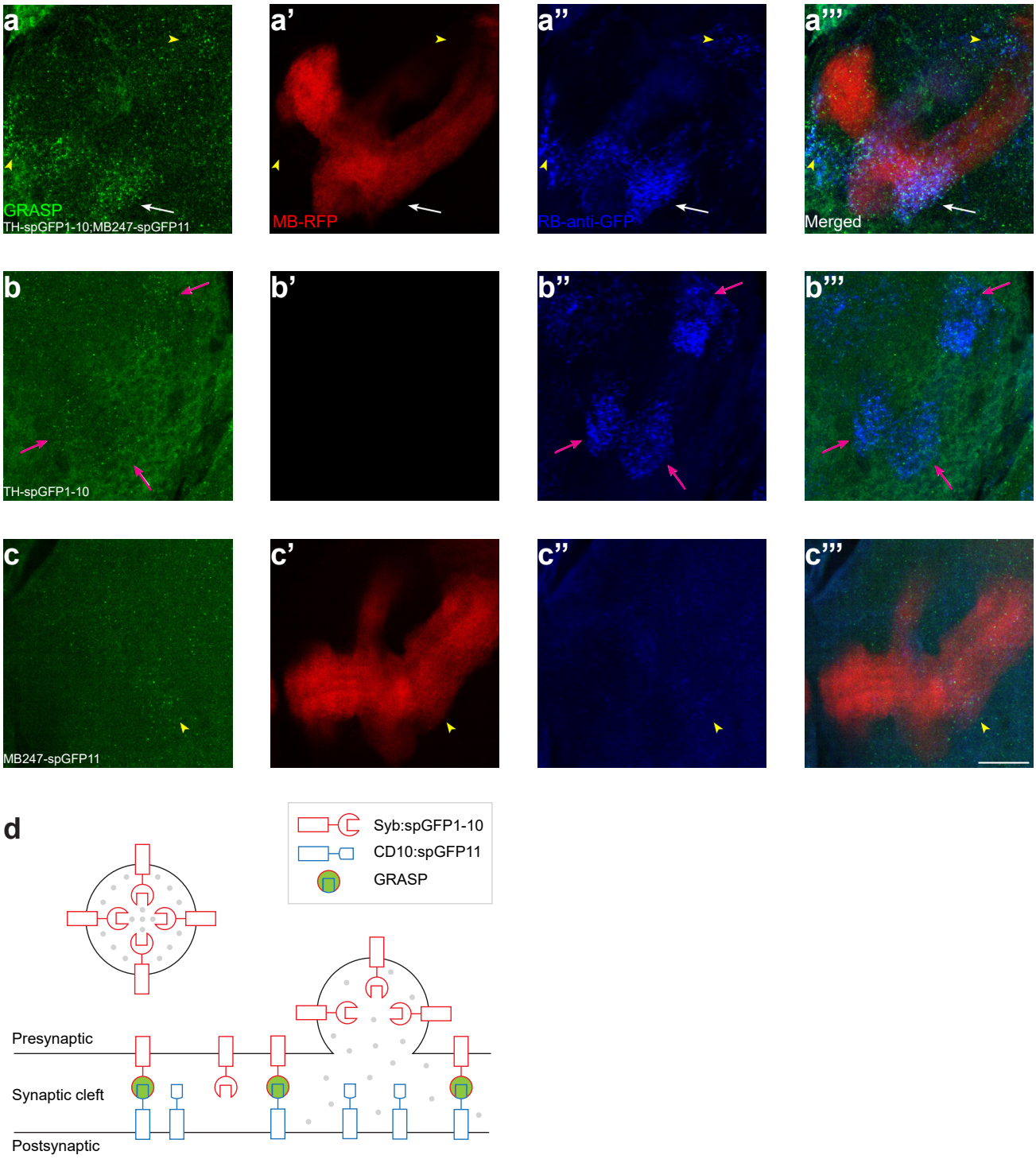
a
GRASP
TH-spGFP1-10:MB247-spGFP11
a'
MB-RFP
a''
RB-anti-GFP
a'''
Merged
b
TH-spGFP1-10
b'
b''
b'''
c
MB247-spGFP11
c'
c''
c'''
d
Syb:spGFP1-10
CD10:spGFP11
GRASP
Presynaptic
Synaptic cleft
Postsynaptic

Figure S2

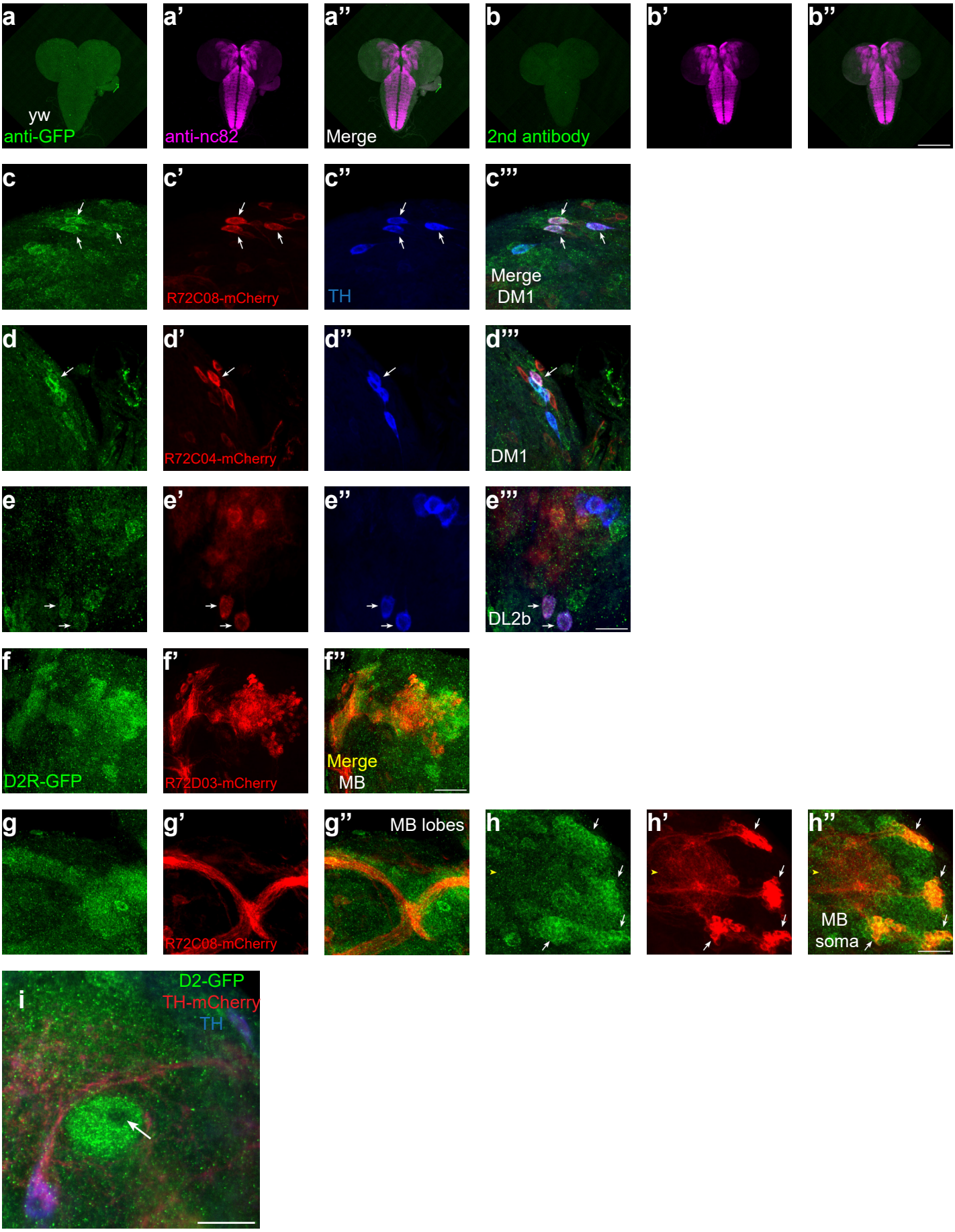
a
yw
anti-GFP
a'
anti-nc82
a''
Merge
b
2nd antibody
b'
b''
c
c'
R72C08-mCherry
c''
TH
c'''
Merge
DM1
d
d'
R72C04-mCherry
d''
d'''
DM1
e
e'
e''
e'''
DL2b
f
D2R-GFP
f'
R72D03-mCherry
f''
Merge
MB
g
g'
R72C08-mCherry
g''
MB lobes
h
h'
h''
MB
soma
i
D2-GFP
TH-mCherry
TH

Figure S3

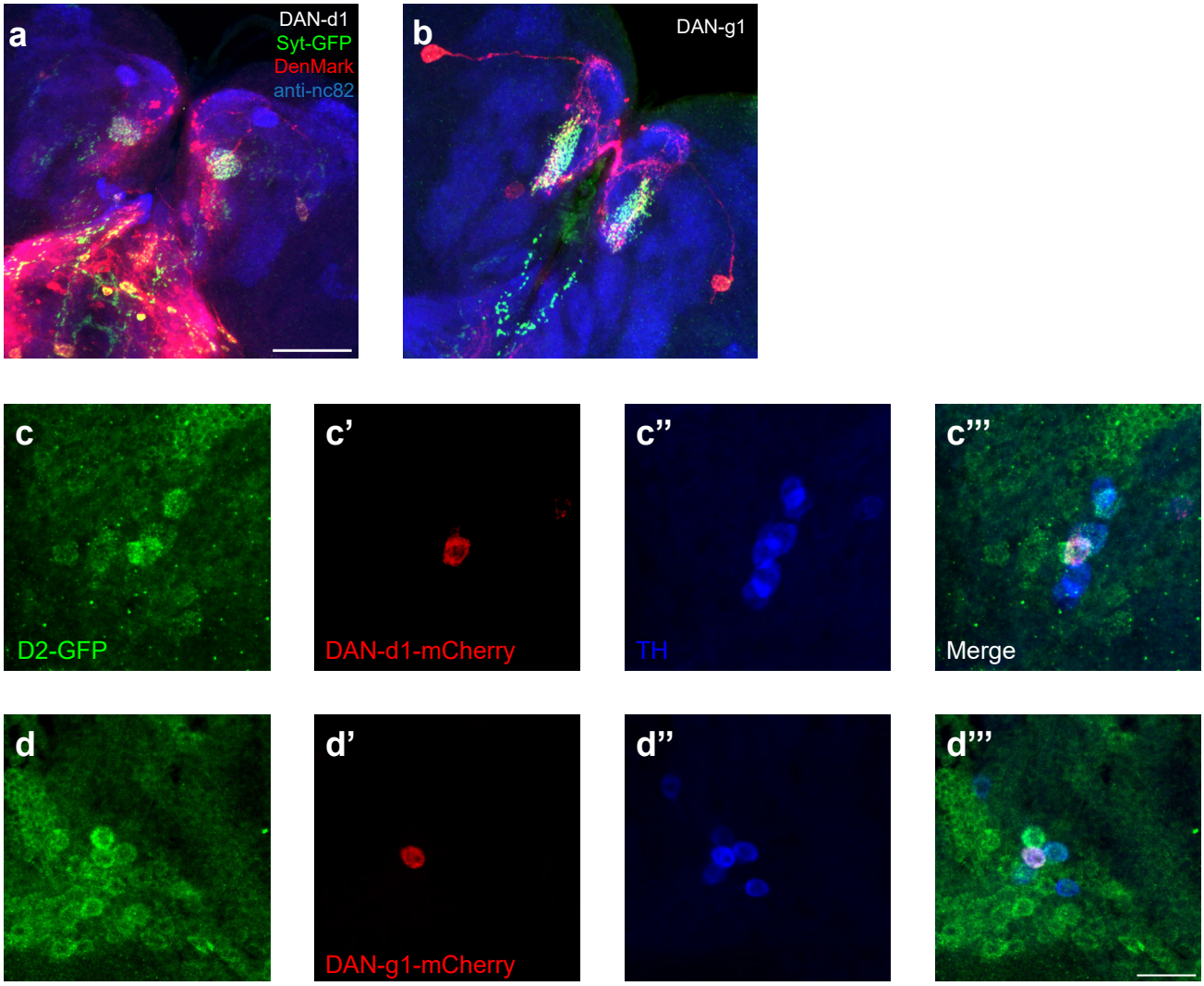
a
DAN-d1
Syt-GFP
DenMark
anti-nc82
b
DAN-g1
c
D2-GFP
c'
DAN-d1-mCherry
c''
TH
c'''
Merge
d
d'
DAN-g1-mCherry
d''
d'''

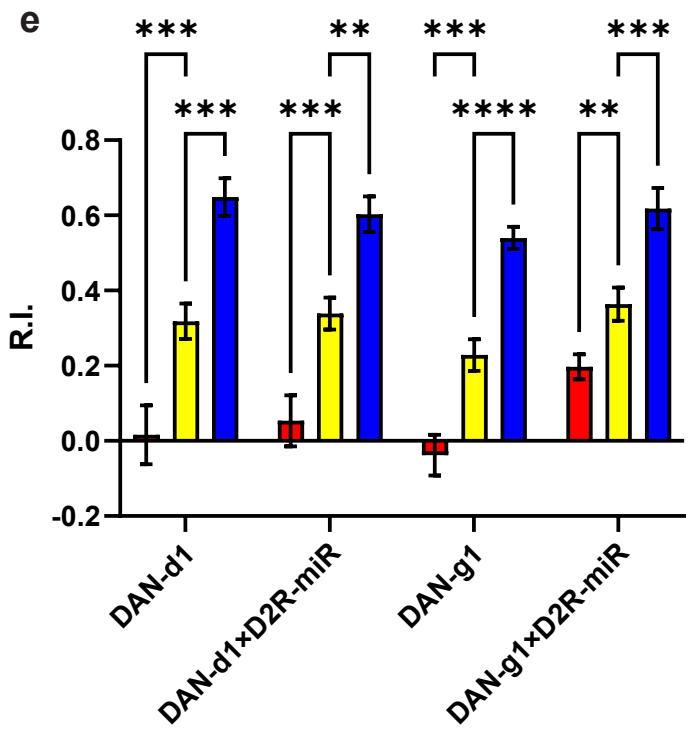
e
R.I.
0.8
0.6
0.4
0.2
0.0
-0.2
***
***
***
**
***
****
***
**
DAN-d1
DAN-d1×D2R-miR
DAN-g1
DAN-g1×D2R-miR

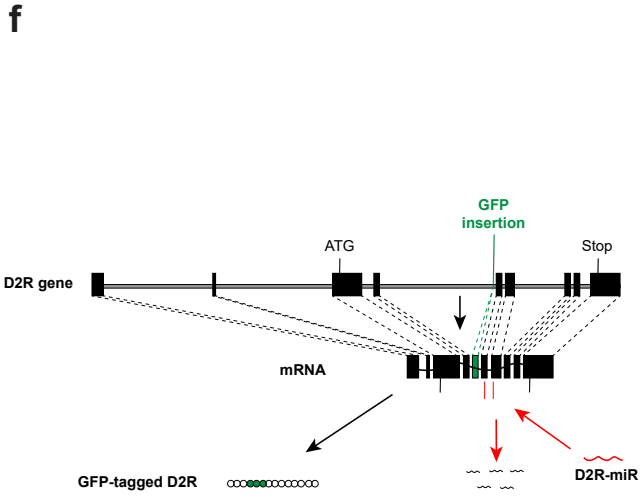
f
D2R gene
ATG
GFP insertion
Stop
mRNA
GFP-tagged D2R
D2R-miR

Figure S4

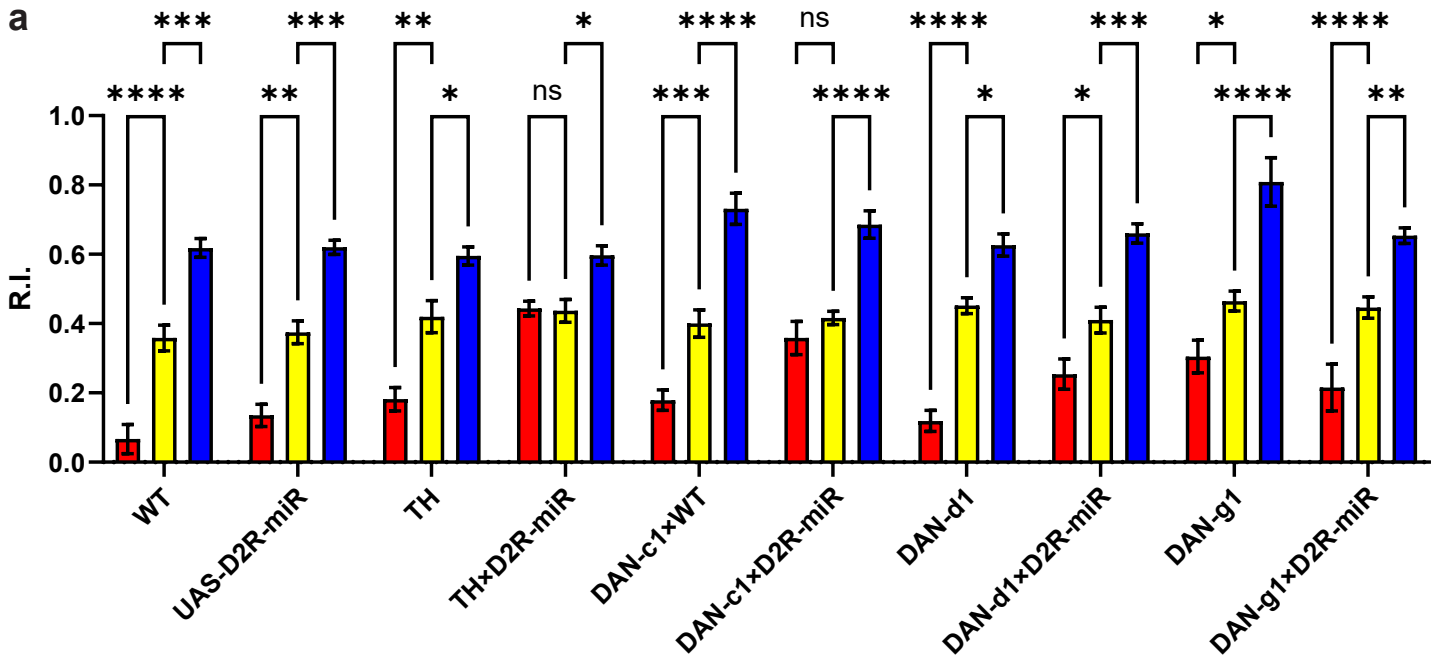
a
R.I.
1.0
0.8
0.6
0.4
0.2
0.0
WT
UAS-D2R-miR
TH
TH×D2R-miR
DAN-c1×WT
DAN-c1×D2R-miR
DAN-d1
DAN-d1×D2R-miR
DAN-g1
DAN-g1×D2R-miR

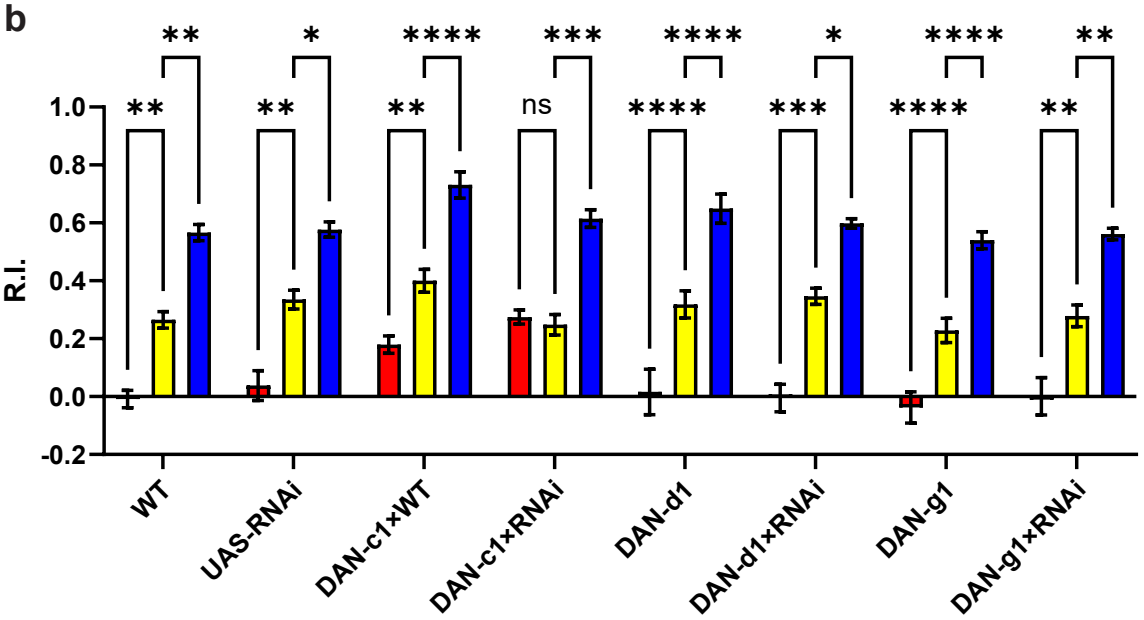
b
R.I.
1.0
0.8
0.6
0.4
0.2
0.0
-0.2
WT
UAS-RNAi
DAN-c1×WT
DAN-c1×RNAi
DAN-d1
DAN-d1×RNAi
DAN-g1
DAN-g1×RNAi

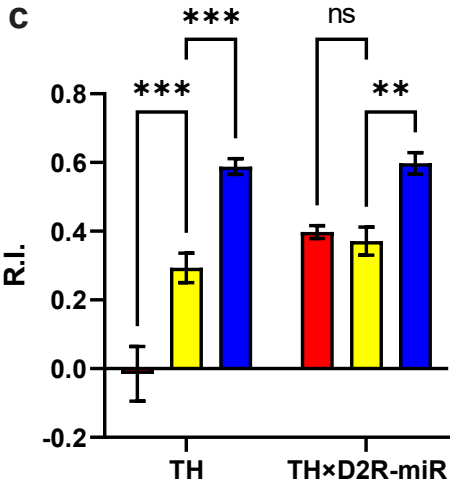
c
R.I.
0.8
0.6
0.4
0.2
0.0
-0.2
TH
TH×D2R-miR

Figure S5

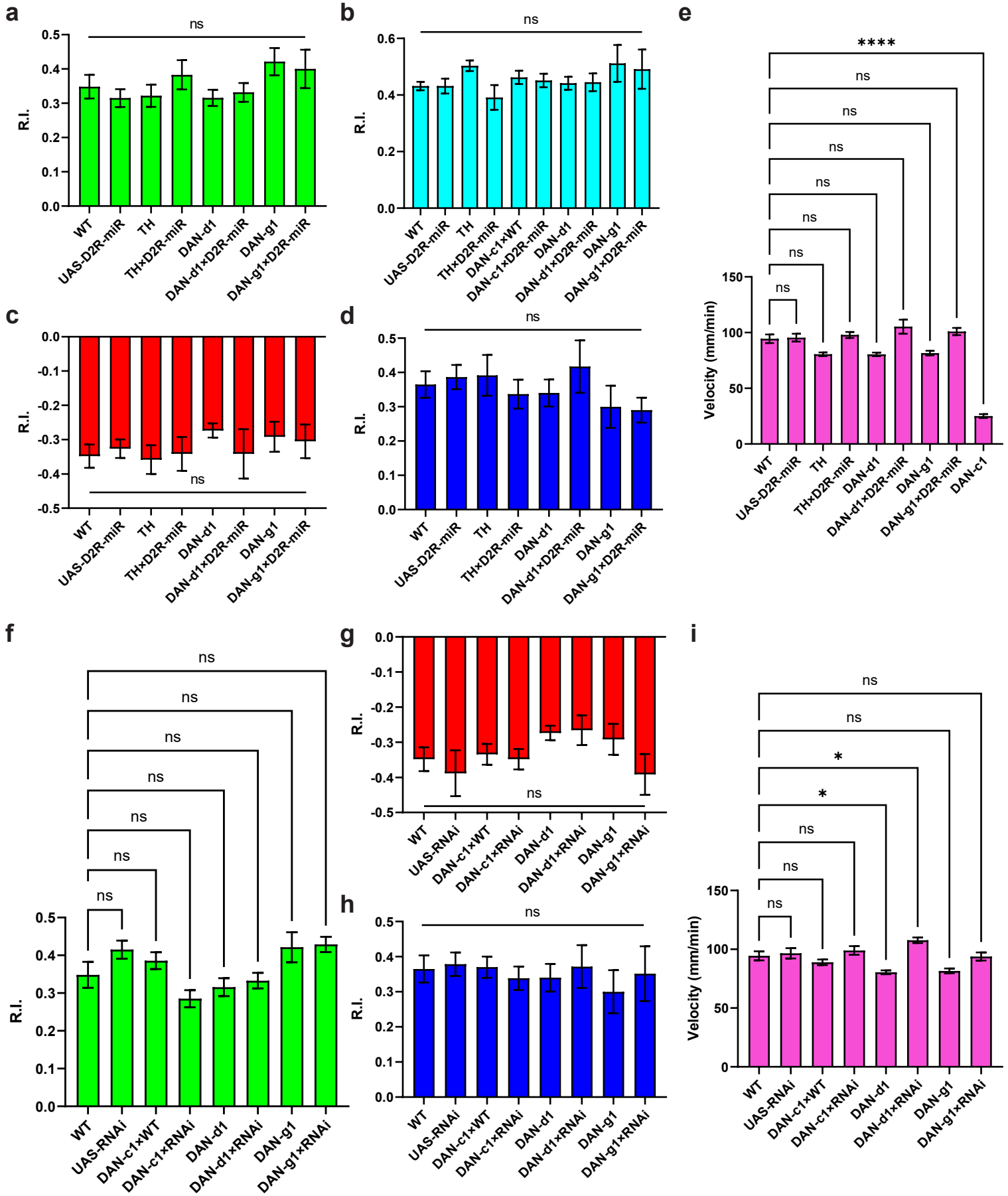
a
R.I.
ns
WT
UAS-D2R-miR
TH
TH×D2R-miR
DAN-d1
DAN-d1×D2R-miR
DAN-g1
DAN-g1×D2R-miR
b
R.I.
ns
WT
UAS-D2R-miR
TH
TH×D2R-miR
DAN-c1×WT
DAN-c1×D2R-miR
DAN-d1
DAN-d1×D2R-miR
DAN-g1
DAN-g1×D2R-miR
e
Velocity (mm/min)
****
ns
WT
UAS-D2R-miR
TH
TH×D2R-miR
DAN-d1
DAN-d1×D2R-miR
DAN-g1
DAN-g1×D2R-miR
DAN-c1
c
R.I.
ns
WT
UAS-D2R-miR
TH
TH×D2R-miR
DAN-d1
DAN-d1×D2R-miR
DAN-g1
DAN-g1×D2R-miR
d
R.I.
ns
WT
UAS-D2R-miR
TH
TH×D2R-miR
DAN-d1
DAN-d1×D2R-miR
DAN-g1
DAN-g1×D2R-miR
f
R.I.
ns
WT
UAS-RNAi
DAN-c1×WT
DAN-c1×RNAi
DAN-d1
DAN-d1×RNAi
DAN-g1
DAN-g1×RNAi
g
R.I.
ns
WT
UAS-RNAi
DAN-c1×WT
DAN-c1×RNAi
DAN-d1
DAN-d1×RNAi
DAN-g1
DAN-g1×RNAi
h
R.I.
ns
WT
UAS-RNAi
DAN-c1×WT
DAN-c1×RNAi
DAN-d1
DAN-d1×RNAi
DAN-g1
DAN-g1×RNAi
i
Velocity (mm/min)
ns
*
WT
UAS-RNAi
DAN-c1×WT
DAN-c1×RNAi
DAN-d1
DAN-d1×RNAi
DAN-g1
DAN-g1×RNAi

Figure S6

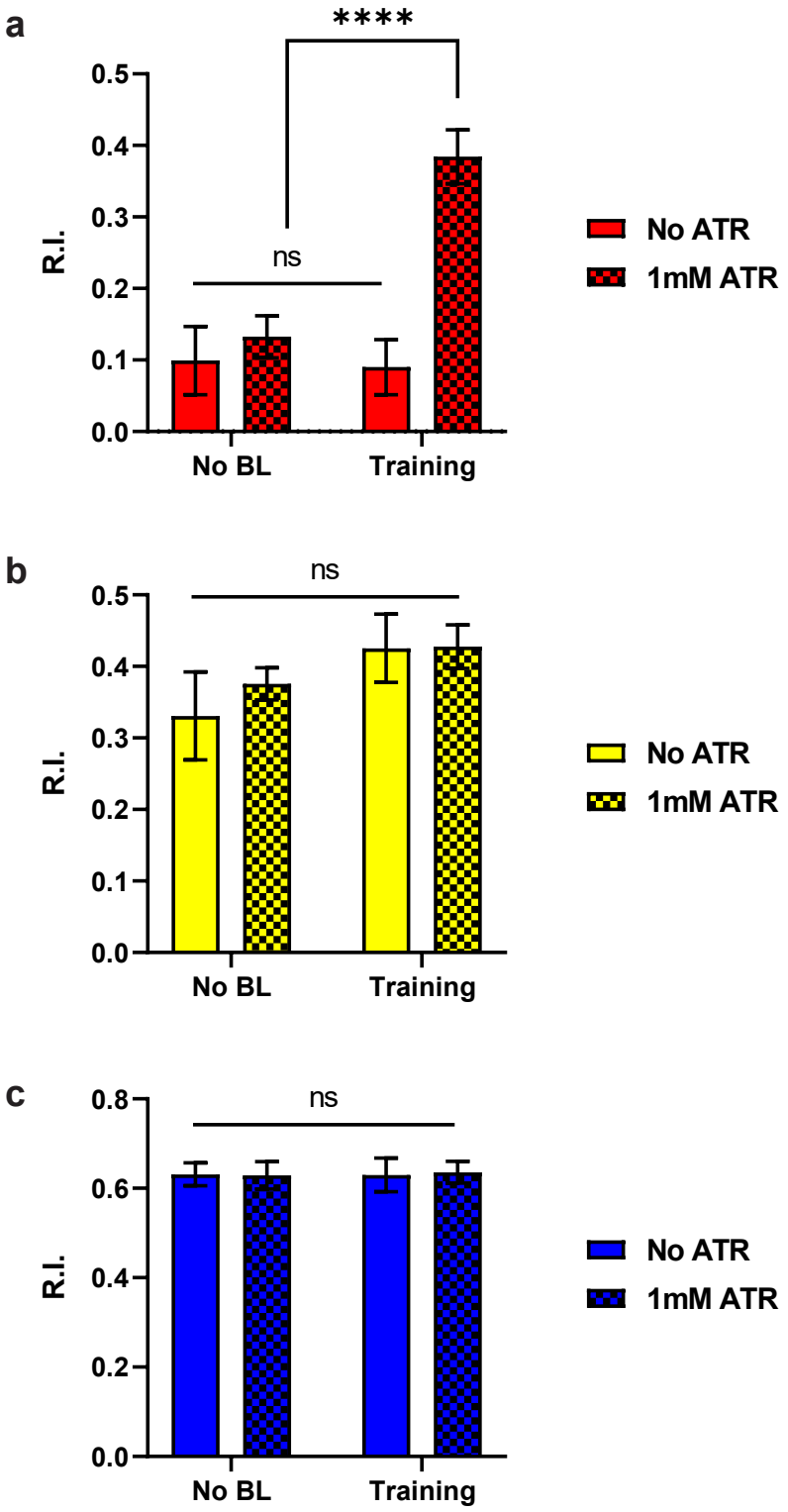
a
****
ns
R.I.
0.5
0.4
0.3
0.2
0.1
0.0
No BL
Training
No ATR
1mM ATR
b
ns
R.I.
0.5
0.4
0.3
0.2
0.1
0.0
No BL
Training
No ATR
1mM ATR
c
ns
R.I.
0.8
0.6
0.4
0.2
0.0
No BL
Training
No ATR
1mM ATR

Figure S7

Table S1

	Strains	Information	Source/Gift	Stock #
1	R72C04	D2R-GAL4 driver (verified)	BDSC	49416
2	R72C08	D2R-GAL4 driver (verified)	BDSC	49621
3	R72D03	D2R-GAL4 driver	BDSC	46676
4	D2R-EGFP	EGFP-tagged D2R	BDSC	60276
5	201Y-GFP	GFP expressed in Mushroom Body	BDSC	64296
6	MB247-LexA::Vp16/TM6B	MB-LexA, mushroom body driver	Dr. M. Gallio's Lab	Macpherson et al. 2015
7	UAS-nSyb-spGFP1-10,LexAop-CD4-spGFP11/CyO	GRASP strain	BDSC	64314
8	LexAop-nSyb-spGFP1-10,UAS-CD4-spGFP11;MKRS/TM6B	Reverse GRASP strain	BDSC	64315
9	WT(Canton-S)	Wild type	BDSC	64349 (1)
10	UAS-RNAi(D2R) (III) line 2	UAS-D2R-RNAi	Dr. A. Kopin's Lab	Draper et al. 2007
11	201Y-GAL4	MB-GAL4, mushroom body driver	BDSC	4440
12	CyO/Sco;TM2,Ubx/TM6,Hu.Tb	Ballancer Chromesome	Dr. S. Tanda's Lab	
13	1407-Gal4	Pan-neuronal driver	BDSC	8751
14	10XUAS-mCD8::GFP (I)	GFP strain	BDSC	32189
15	10XUAS-mCD8::GFP (II)	GFP strain	BDSC	32186
16	10XUAS-mCD8::GFP (III)	GFP strain	BDSC	32184
17	UAS-ChR2; UAS-ChrR2	Optogenetics strain	Dr. B. Condron's Lab	
18	LexAop-rCD2::RFP; UAS-CD4-spGFP1-10, LexAop-CD4-spGFP11	RFP expressed in MB; GRASP	BDSC	58755
19	UAS-CD8::mCherry (II)	mCherry strain	BDSC	27391
20	UAS-CD8::mCherry (III)	mCherry strain	BDSC	27392
21	yw1118	Wild type for D2R-EGFP	Dr. S. Tanda's Lab	
22	D2R-miR	UAS-DD2R-microRNA	Dr. M. Wu's Lab	Xie et al. 2018
23	UAS-*Shibirets1*	Thermogenetics strain	Dr. T. Kitamoto's Lab	
24	UAS-dTRPA1	Thermogenetics strain	BDSC	26263
25	UAS-nsyb::GFP; UAS-DenMark	Pre- and postsynaptic terminals	BDSC	33056

Table S2

	22°C			34°C		
	QUI	**DW**	**SUC**	**QUI**	**DW**	**SUC**
shibire^{ts1}	9	8	8	9	9	9
DAN-c1×shibire^{ts1}	14	6	7	17	6	9
DAN-c1	8	9	9	9	9	9
DAN-c1×dTRPA1	15	14	13	14	15	13
dTRPA1	9	8	9	10	10	10

Table S3

Driver	Cross	Pentyl acetate (PA)			Propionic acid (P-A)			Naïve olfactory		Naïve gustatory		Locomotion
		QUI	DW	SUC	QUI	DW	SUC	PA	P-A	QUI	SUC	
TH ×	miR	8	8	8	6	6	6	7	7	6	6	24
	RNAi	-	-	-	-	-	-	-	-	-	-	-
	CR	8	6	6	6	6	6	6	6	6	6	12
DAN-c1 ×	miR	38	38	37	14	13	14	12	8	11	12	50
	RNAi	6	6	6	-	-	-	8	-	6	6	24
	CR	14	10	10	11	8	8	12	9	11	12	36
DAN-d1 ×	miR	17	15	13	8	8	7	6	6	6	7	16
	RNAi	6	6	6	-	-	-	7	-	7	6	16
	CR	13	11	10	9	6	6	7	6	6	6	15
DAN-g1 ×	miR	31	22	16	13	8	8	8	8	6	7	22
	RNAi	8	8	6	-	-	-	8	-	6	7	24
	CR	23	19	18	8	8	7	8	6	6	6	15
201Y ×	miR	7	7	8	6	6	6	6	6	6	6	24
	RNAi	-	-	-	-	-	-	-	-	-	-	-
	CR	6	6	6	6	6	6	6	6	6	6	24
WT		6	6	6	6	6	6	6	6	6	6	24
D2R-miR		12	12	12	6	6	6	12	6	11	12	36
RNAi		6	6	6	-	-	-	6	-	6	6	20

Table S4

Strains	Groups	BL									No BL		
		Resting			Learning			Testing					
		QUI	DW	SUC	QUI	DW	SUC	QUI	DW	SUC	QUI	DW	SUC
TH×ChR2	ATR	-	-	-	21	13	10	-	-	-	20	16	10
	No ATR	-	-	-	16	13	8	-	-	-	14	13	8
DAN-c1×ChR2	ATR	11	8	9	15	12	9	9	8	8	16	11	9
	No ATR	9	9	8	15	12	8	9	9	9	16	12	9
201Y×ChR2	ATR	8	7	7	9	6	9	7	7	10	11	8	7
	No ATR	10	7	7	10	7	7	9	7	13	12	10	7